DE GRUYTER OPEN

Research Article

Open Access

D. A. Hadjiloizi, A. L. Kalamkarov, Ch. Metti, and A. V. Georgiades*

Analysis of Smart Piezo-Magneto-Thermo-Elastic Composite and Reinforced Plates: Part II – Applications

Abstract: A comprehensive micromechanical model for the analysis of a smart composite piezo-magneto-thermo-elastic thin plate with rapidly varying thickness is developed in Part I of this work. The asymptotic homogenization model is developed using static equilibrium equations and the quasi-static approximation of Maxwell's equations. The work culminates in the derivation of general expressions for effective elastic, piezoelectric, piezomagnetic, dielectric permittivity and other coefficients. Among these coefficients, the so-called product coefficients are determined which are present in the behavior of the macroscopic composite as a result of the interactions between the various phases but can be absent from the constitutive behavior of some individual phases of the composite structure. The model is comprehensive enough to also allow for calculation of the local fields of mechanical stresses, electric displacement and magnetic induction. The present paper determines the effective properties of constant thickness laminates comprised of monoclinic materials or orthotropic materials which are rotated with respect to their principal material coordinate system. A further example illustrates the determination of the effective properties of wafer-type magnetoelectric composite plates reinforced with smart ribs or stiffeners oriented along the tangential directions of the plate. For generality, it is assumed that the ribs and the base plate are made of different orthotropic materials. It is shown in this work that for the purely elastic case the results of the derived model converge exactly to previously established models. However, in the more general case where some or all of the phases exhibit piezoelectric and/or piezomagnetic behavior, the expressions for the derived effective coefficients are shown to be dependent on not only the elastic properties but also on the piezoelectric and piezomagnetic parameters of the constituent materials. Thus, the results presented here represent a significant refinement of previously obtained results.

Keywords: smart composite piezo-magneto-thermo-elastic thin plate; asymptotic homogenization; effective properties; product properties

1 Introduction

The incorporation of composites and, more recently, nanocomposites, into new engineering applications has been restricted to some extend by the lack of a reliable data-base of their long-term performance characteristics under different loading conditions. This problem has been offset to a significant degree by the recent development and optimization of elaborate sensor and actuator systems. On one hand, sensors can provide valuable data on the current state and serviceability of the structure and on the other hand the actuators can respond effectively to changes in external conditions/stimuli such as mechanical loading, electric and magnetic field intensity, temperature etc. To enhance a structure's ability to fulfill the re-

*Corresponding Author: A. V. Georgiades: Department of Mechanical Engineering and Materials Science and Engineering, Cyprus University of Technology, Limassol, Cyprus
and Research Unit for Nanostructured Materials Systems, Department of Mechanical Engineering and Materials Science and Engineering, Cyprus University of Technology, Limassol, Cyprus; E-mail: Tasos.Georgiades@cut.ac.cy; Tel.: 357-25002560
D. A. Hadjiloizi: Department of Mechanical Engineering and Materials Science and Engineering, Cyprus University of Technology, Limassol, Cyprus
and Research Unit for Nanostructured Materials Systems, Department of Mechanical Engineering and Materials Science and Engineering, Cyprus University of Technology, Limassol, Cyprus
A. L. Kalamkarov: Department of Mechanical Engineering, Dalhousie University, PO Box 15000, Halifax, Nova Scotia, B3H 4R2, Canada
Ch. Metti: Department of Mechanical Engineering and Materials Science and Engineering, Cyprus University of Technology, Limassol, Cyprus
and Research Unit for Nanostructured Materials Systems, Department of Mechanical Engineering and Materials Science and Engineering, Cyprus University of Technology, Limassol, Cyprus

quirements of a particular engineering application and guarantee long-term reliability and sustenance, it is necessary to integrate composites/nanocomposites with the aforementioned sensors/actuators; this gives rise to smart composites and smart nanocomposites, see for example Kalamkarov et al. [1]. Jain and Sirkis [2] aptly compared smart structures to biological systems. In their work they defined the goal of smart structures as being able to reproduce biological functions in load-bearing mechanical systems; thus smart structures should be endowed with a "skeletal system" to provide load-bearing capabilities, a "nervous system", which is a system of integrated sensors or actuators to assess the structural health state, a "motor system" to provide adaptive response, an "immune system" for self-healing capabilities and a "neural system" for promoting learning and decision making [2]. Suitable candidates for use as sensors and actuators in smart composite materials systems include electro/magneto-rheological fluids, shape-memory alloys, piezomagnetics and magnetostrictives, piezoelectrics and others.

Of particular interest among smart materials are those consisting of piezoelectric and piezomagnetic constituents. Such magnetoelectric composites have attracted attention both because of their significant potential for engineering applications as well as the unique properties they exhibit. In particular, magnetoelectric composites are primarily characterized by the so-called product properties which are present in the behavior of the overall macroscopic structure but are usually absent from the constitutive behavior of the individual constituents, see Newnham et al. [3], Nan et al. [4]. Examples of product properties are the magnetoelectric effect, pyromagnetism and pyroelectricity. According to Nan et al. [4] we can succinctly write the product properties as follows:

$$\text{Magnetoelectric Effect} = \frac{\text{Magnetic}}{\text{Mechanical}} \times \frac{\text{Mechanical}}{\text{Electric}}$$

$$\text{Pyroelectric Effect} = \frac{\text{Thermal}}{\text{Mechanical}} \times \frac{\text{Mechanical}}{\text{Electric}}$$

$$\text{Pyromagnetic Effect} = \frac{\text{Thermal}}{\text{Mechanical}} \times \frac{\text{Mechanical}}{\text{Magnetic}}$$

Thus, applying an electric field to a magnetoelectric composite generates mechanical displacement in the piezoelectric phase. Provided there is a satisfactory degree of bonding between the different constituents, this mechanical deformation is transferred to the piezomagnetic phase and in turn induces a magnetic field. Thus, overall, an applied electric field generates a magnetic field and, conversely, an applied magnetic field produces electric displacement. This is the magnetoelectric phenomenon. Similarly, changing the temperature produces mechanical strain through thermal expansion. In turn this strain generates magnetic induction in the piezomagnetic phase (py-

romagnetism) and electric displacement (pyroelectricity) in the piezoelectric phase.

As a result of their unique properties magnetoelectric composites are continuously coming into the forefront of an increasing number of engineering applications. Typical examples include resonators, phase shifters, delay lines and filters, magnetic field sensors, energy harvesting transducers, miniature antennas, data storage devices and spintronics, biomedical sensors for EEG/MEG devices and other relevant equipment, see [5–14].

The incorporation of smart materials and, particularly, magnetoelectric composites into new engineering applications is significantly facilitated if their properties and coefficients can be predicted at the design stage; thus micromechanical models are needed. These models must be comprehensive enough to capture both the individual behavior of the different constituents as well as the influence of the macroscopic composite. At the same time, if the developed models are too complicated to be used in an effective and efficient manner then they are of little use beyond the obvious academic interest. Ideally, these models should lead to closed-form design-oriented equations that can be programmed into a simple spread-sheet. That way they can facilitate engineering analysis to obtain a preliminary design and, if any fine-tuning is needed, the designer can turn to a numerical model based on, for example, the finite element technique. To this end, the main objective of this work is the development of multiphysics micromechanical models for the analysis and design of thin piezo-magneto-thermo-elastic composite and reinforced plate structures. The nature of the developed models is such that they permit the designer to readily customize the effective properties of a given smart structure by varying one or more geometrical or material parameters such as the stacking sequence in a magnetoelectric laminate, thickness and composition of the perpendicular ribs of wafer-reinforced plates etc.

Among the earlier works on magnetoelectric composites are those of Harshe et al. [15, 16] and Avelaneda and Harshe [17], who developed theoretical models to determine the magnetoelectric coefficients of 0-3 and 2-2 piezoelectric-magnetostrictive multilayer composites. However, deviations are observed between their results and corresponding experimental values. Osaretin and Rojas [18] purport that this discrepancy could be attributed to poor interface coupling between the layers, as far as the experimental results are concerned, and failure to properly incorporate the appropriate electromagnetic boundary conditions as far as the theoretical models are concerned. The authors then go on to develop a different modeling methodology by solving the constitutive equations in

each phase and then applying a field-averaging method, see e.g. Getman [19], with pertinent boundary conditions, to obtain the composite effective properties. Their results agree with their counterparts from other theoretical models such as the one developed by Nan [20], who employed a Green's Function approach. However, a discrepancy with experimental results still remained which was corrected by applying an interface coupling parameter of 0.4 (logical from a practical point of view) to the theoretical model. Particularly noteworthy are the works of Huang and collaborators, [21, 23, 24]. In particular, Huang and Kuo [21] developed a comprehensive micromechanical model for piezoelectric-piezomagnetic composites containing ellipsoidal inclusions. As in most other theoretical models, the authors assumed perfect bonding between the inclusion and the matrix and ignored any other interfacial defects. Their modeling methodology allowed them to obtain the coupled magneto-electro-elastic analogue of the Eshelby tensors [22] which, as expected, are a function of the geometric characteristics of the ellipsoidal inclusions as well as the properties of the host matrix. In an extension of this work, Huang [23] obtained closed-form solutions for reinforcements in the shape of elliptic cylinders, circular cylinders, disks and ribbons embedded in a transversely isotropic matrix. Other related work on magnetoelectric composites consisting of long piezoelectric fibers embedded in a piezomagnetic matrix can be found in [24].

Hadjiloizi et al. [25, 26] employed the asymptotic homogenization technique to develop two general three-dimensional models for magnetoelectric composites. One model used dynamic force and thermal balance and the time-varying form of Maxwell's equations to determine closed-form expressions for the complete set of the effective properties of the structure including electrical conductivity and the product properties. The second model used the quasi-static approximation of the aforementioned constitutive equations. The models were applied to the case of thick laminates. It was shown that the results of the quasi-static model agreed with those of other models, see for example Bravo-Castillero et al [27]. Ni et al [28] examined the effect of the orientation of the applied electric and magnetic fields on the magnetoelectric coupling of polycrystalline multiferroic laminates. The authors based their theoretical model on a three-layer sandwich laminate consisting of a polycrystalline piezoelectric layer between two piezomagnetic laminae. Their model assumed the application of dc poling electric and magnetic fields because the constituent materials do not exhibit an appreciable degree of electromechanical and magnetomechanical behavior in their unpoled states. In the model an ac magnetic field, δH_j, is applied and the induced polariza-

tion, δP_i, is calculated. The effective magnetoelectric coefficients were then calculated as $a_{ij} = \delta P_i / \delta H_j$. The model showed that these coefficients depended on the sum of the in-plane piezomagnetic strains, $\varepsilon_{11} + \varepsilon_{22}$, which in turn depended strongly on the orientation of the applied magnetic fields relative to the laminate's interface. Tsang et al. [29] developed an effective medium-based micromechanical model for 3-phase magnetoelectric composites consisting of spherical magnetostrictive and piezoelectric particles embedded in a conductive polymer matrix. Based on their model, the authors calculated the magnetoelectric charge and voltage coefficients, and the results agreed reasonably well with corresponding experimental data. In their modeling approach, Pan et al. [30] transformed a cylindrical layered composite, consisting of piezoelectric and piezomagnetic laminae, into an equivalent planar one. This modeling approach proved useful in the analysis and design of magnetoelectric devices and structures. Bichurin et al. [31] developed a micromechanical model pertaining for ferromagnetic/piezoelectric bilayered and multilayered composites with the electric and magnetic fields applied in varying orientations with respect to the laminates' interface. Longitudinal and transverse magnetoelectric coefficients were calculated. Regarding the former coefficient, the authors illustrated that earlier results [15] were a limiting case of their theory. The same authors, Bichurin et al. [32], extended their work to magnetoelectric nanocomposites. Other relevant results can be found in the works of Akhabarzadeh et al. [33], Soh and Liu [34], Kirchner et al. [35], Pan and Heyliger [36], Benveniste [37], Spyropoulos et al. [38], Tang and Yu [39, 40] and others.

The constitutive and governing equations describing the micromechanical behavior of periodic composites and smart composites (including the magnetoelectric composites that are of interest to us in this work) are characterized by rapidly varying material coefficients. In other words, the material coefficients are periodic with a small period, of the order of a few micrometers or nanometers. This spatial scale is typically portrayed in literature as the microscopic or "fast" scale. Superimposed on this scale however, one encounters a macroscopic or "slow" scale, which is a function of the global formulation of the problem (external loads, boundary conditions etc.) and is "oblivious" to the substructural phenomena that take place at the level of the reinforcement or general inclusion. Consequently, any attempt to solve a problem related to a smart composite must successfully decouple the two scales and treat the two problems (macroscopic and microscopic) independently. One such technique that has enjoyed significant success for many years is that of asymptotic homogenization. The pertinent mathematical details

of the technique can be found in Bensoussan et al. [41], Sanchez-Palencia [42], Bakvalov and Panasenko [43] and Cioranescu and Donato [44]. Many problems in elasticity, thermoelasticity, and piezo-magneto-elasticity have been solved via asymptotic homogenization. We want to mention particularly the works of Kalamkarov [45], who analyzed a wide variety of problems, such as composite and reinforced plates and shells, network-reinforced shells, plates with corrugated surfaces and other structures, Kalamkarov and Kolpakov [46] who used these models to design and optimize various composite structures on account of strength and stiffness requirements, the pioneering work of Guedes and Kikuchi [47] on computational aspects of homogenization, the modification of asymptotic homogenization for problems related to elasticity and thermal conductivity of thin plates appearing in the works of Duvaut [48, 49], Andrianov et al. [50, 51], Caillerie [52, 53], Kohn and Vogelius [54–56] and many others.

Recent years have witnessed the emergence of smart composite plates and shells as the preeminent structural members for many practical applications. Enhanced strength, reduced weight, materials savings and ease of fabrication are among the reasons that make these structures attractive. More recently, advancements in the field of nanotechnology and the increasing popularity of nanocomposite thin films, plates and shells [57] have further enhanced the application potential of such structures. The periodic or nearly periodic nature of smart composite and nanocomposite plates and shells renders asymptotic homogenization a valuable tool in their analysis, design and optimization.

The "classical" asymptotic homogenization approach however cannot be applied directly to a thin plate or shell if the scale of the spatial inhomogeneity is comparable to the thickness of the structure. In that case, a refined approach developed by Caillerie [52, 53] in his heat conduction studies is needed. In particular, a two-scale formalism is applied, whereby a set of microscopic variables is used for the tangential directions in which periodicity exists and another microscopic variable is used for the transverse direction in which periodicity considerations do not apply. Kohn and Vogelius [54–56] adopted this approach in their study of the pure bending of a thin, linearly elastic homogeneous plate. Kalamkarov [45] and Kalamkarov and Kolpakov [46] applied this modified two-scale methodology to determine the effective elastic, thermal expansion and thermal conductivity coefficients of thin curvilinear composite layers. Challagulla et al. [58], Georgiades et al. [59] employed this methodology to develop comprehensive asymptotic homogenization models for network-reinforced thin smart composite shells. These

authors illustrated their results by means of practically important examples including single-walled carbon nanotubes, which can be treated as network-reinforced composite shells in which the covalent bonds between the carbon atoms play the role of isotropic reinforcements embedded in a matrix of zero rigidity. Kalamkarov and Georgiades [60] and, Georgiades and Kalamkarov [61] developed comprehensive micromechanical models for smart composite wafer- and rib-reinforced plates. Saha et al. [62] determined the effective elastic constants of orthotropic honeycomb-like sandwich composite shells. Hadjiloizi et al. [63] implemented a general model (based on the time-varying form of Maxwell's equations and dynamic force balance) for the micromechanical dynamic analysis of magnetoelectric thin plates with rapidly varying thickness. In that work only an in-plane temperature variation was considered and therefore any out-of-plane thermal effects were ignored. Thus, unlike in the present work, the out-of-plane thermal expansion, pyroelectric and pyromagnetic coefficients were not captured in [63]. More important, however, is the fact that the micromechanical model in [63] is only applied to the case of simple laminated plates. In contrast, the model developed in the present work explicitly allows for different periodicity in the lateral directions. As such, it is readily amenable to the design and analysis of magnetoelectric reinforced plates such as the wafer-reinforced structures shown in Section 4. To the authors' best knowledge, this is the first time completely coupled piezo-magneto-thermo-elastic effective coefficients for reinforced plates are presented and analyzed.

Also relevant to the present papers are the works of Kalamkarov and Georgiades [60], Georgiades and Kalamkarov [61] and Hadjiloizi et al. [25], [26]. In [60] and [61], Kalamkarov and Georgiades developed and illustrated the use of an asymptotic homogenization model for the analysis of reinforced piezoelectric plates. In their work, [60], [61] the authors adopted only a semi-coupled analysis, which results in expressions for the effective coefficients that do not reflect the influence of such parameters as the electric permittivity, magnetic permeability, primary magnetoelectricity etc. In the present work and its companion paper [64], however, a fully coupled analysis is performed, and as a consequence the expressions for the effective coefficients involve all pertinent material parameters. As an example, the effective extensional elastic coefficients are dependent on not only the elastic properties of the constituent materials, but also on the piezoelectric, piezomagnetic, magnetic permeability, dielectric permittivity and magnetoelectric coefficients. The same holds true for the remaining effective coefficients. In

a sense, the thermoelasticity, piezoelectricity and piezomagnetism problems are entirely coupled, and the solution of one affects the solutions of the others. This feature is captured in the present papers, but not in previously published works, such as [60] and [61]. Thus, the results presented here represent an important refinement of previously established results. To the authors' best knowledge completely coupled piezo-magneto-thermo-elastic effective coefficients for reinforced plates have not been presented and analyzed before.

In [25], [26], Hadjiloizi et al. developed general quasistatic and dynamic three-dimensional models for magnetoelectric composites. However, these models employed the "classical" homogenization approach, see [43] for example, and consequently could not capture the mechanical, thermal, piezoelectric and piezomagnetic behavior that is related to bending, twisting and general out-of-plane deformation and electric and magnetic field generation. The model developed in the current work and its companion paper [64], however, accomplishes precisely this; it employs the modified asymptotic homogenization technique (discussed earlier) which makes use of two sets of microscopic variables that permit the decoupling of in-plane and out-of-plane behavior of the structure under consideration. For example, the elastic coefficients can be distinguished into the familiar extensional, bending and coupling coefficients, which is not possible to achieve with the 3D models in [25] and [26]. What this amounts to is the fact that the two modeling approaches are essentially applicable to entirely different structures and geometries. The 3D models in [25], [26] can be used to analyze structures of comparable dimensions in the x, y, z directions (such as *thick* laminates) but cannot be used for thin structures such as wafer- and rib-reinforced plates. The micromechanical models developed in the present work, however, are applicable to structures with a much smaller dimension in the transverse direction than in the other two directions. Thus, they can be used in the design and analysis of an impressive range of composite and reinforced plates such as the aforementioned wafer- and rib-reinforced structures (see Section 4), three-layered honeycomb-cored magnetoelectric plates, *thin* laminates (Section 3) etc.

To summarize, the present paper deals with the development and applications of appropriate plane stress micromechanical models for thin magnetoelectric composite and reinforced plates. The work is implemented in two parts. In part I [64] the pertinent micromechanical models are derived, and the unit cell problems, from which the effective coefficients (including the product properties) can be extracted, are obtained. The applications of the developed models to the practically important cases of thin composite laminates and wafer-reinforced magnetoelectric plates are presented herein. Following this introduction the basic mathematical model and the pertinent unit cell problems are reviewed in Section 2. Sections 3 and 4 present, respectively, the solution of the unit cell problems for magnetoelectric laminates of constant thickness and for wafer-reinforced magnetoelectric plates. Section 4 also compares the results of the developed model with previously reported results, and, finally, Section 5 concludes the work.

In view of the applications mentioned earlier in this section, the most important aspect of this publication is the development of closed-form design-oriented equations that can be used in the analysis and design of magnetoelectric composite and reinforced plates. It is shown that thermoelasticity, piezoelectricity and piezomagnetism are entirely coupled and the solution of one affects the solutions of the others.

2 Problem Formulation

The boundary value problem characterizing the thin smart composite plate of rapidly varying thickness, Fig. 1 in Hadjiloizi et al. [64], is given by:

$$\sigma_{ij,jx} = P_i, \quad D_{i,ix} = 0, \quad B_{i,ix} = 0$$
$$E_i = -\varphi_{,ix}, \quad H_i = -\psi_{ix} \tag{2.1a}$$

$$\sigma_{ij}n_j = p_i, \quad D_i n_i = 0, \quad B_i n_i = 0, \quad \text{on } S^{\pm}$$
$$u_i = 0, \quad \varphi = \delta^2 e, \quad \psi = \delta^2 h, \quad \text{on lateral surfaces} \tag{2.1b}$$

$$\sigma_{ij} = C_{ijkl}u_{k,xl} + e_{kij}\varphi_{,xk} + Q_{kij}\psi_{,xk} - \delta\Theta_{ij}T$$
$$D_i = \delta\left\{e_{ijk}u_{k,xl} - \varepsilon_{ij}\varphi_{,xk} - \lambda_{ij}\psi_{,xk} + \delta\xi_i T\right\}$$
$$B_i = \delta\left\{Q_{ijk}u_{k,xl} - \lambda_{ij}\varphi_{,xk} - \mu_{ij}\psi_{,xk} + \delta\eta_i T\right\} \tag{2.2a}$$

In these equations we use the following short-hand notation for the derivatives:

$$\frac{\partial\varphi_\alpha}{\partial y_\beta} = \varphi_{\alpha,\beta y}, \quad \frac{\partial\varphi_\alpha}{\partial x_\beta} = \varphi_{\alpha,\beta x}, \quad \frac{\partial\varphi_\alpha}{\partial z} = \varphi_{\alpha,z} \tag{2.2b}$$

Here σ_{ij} is the mechanical stress, D_i and B_i are, respectively, the electric displacement and magnetic induction, E_i and H_i are the electric and magnetic fields, P_i represents a generic body force, p_i represents the surface tractions, and u_i is the mechanical displacement. Finally, T is the change in temperature with respect to a suitable reference. Eq. 2.1a represents the static equilibrium equations

and the quasi-static approximation of Maxwell's Equations. The irrotational electric and magnetic fields can be expressed as gradients of scalar potential functions, φ and ψ, respectively. Furthermore, $e_{kl} = \partial u_k / \partial x_l$ is the second order strain field, C_{ijkl}, e_{ijk}, Q_{ijk}, and Θ_{ij} are the tensors of the elastic, piezoelectric, piezomagnetic and thermal expansion coefficients respectively. Finally, ε_{ij}, λ_{ij}, μ_{ij}, ξ_i and η_i represent, respectively, the dielectric permittivity, the magnetoelectric coefficients, the magnetic permeability, and the pyroelectric and pyromagnetic tensors. We note that because the composite layer is periodic only in the tangential directions, see Fig. 1 of Hadjiloizi et al [64], the material parameters are dependent on x_α / δ_{ha} and x_3, while the dependent field variables are also dependent on $x_\alpha = (x_1, x_2)$. In all equations we adopt the convention that Greek letters, α, β, γ etc. assume values of only 1,2, while Latin letters, a, b, c etc. take on values 1,2,3. We finally note that the overall thickness of the structure must be small compared to the other two dimensions. For the analysis of a thick piezo-magneto-thermo-elastic laminate, one should consider an appropriate 3D model, e.g. [25, 27].

The in-plane force and moment resultants pertaining to the homogenized plate are given in Hadjiloizi et al. [64] and are:

$$N_{\alpha\beta} = \delta \left\langle b_{\alpha\beta}^{\mu\nu} \right\rangle \varepsilon_{\mu\nu} - \delta^2 \left\langle b_{\alpha\beta}^{(1)\mu\nu} \right\rangle u_{3,x_\mu x_\nu}^{(0)} +$$
$$+ \delta \left\langle b_\mu^{\alpha\beta} \right\rangle \varphi_{,x_\mu}^\star + \delta \left\langle a_\mu^{\alpha\beta} \right\rangle \psi_{,x_\mu}^\star \delta^2 \left\langle b_{\alpha\beta} \right\rangle T_1^{(0)} +$$
$$+ \delta^2 \left\langle b_{\alpha\beta}^{(1)} \right\rangle T_2^{(0)}$$

(2.3a)

$$M_{\alpha\beta} = \delta^2 \left\langle z b_{\alpha\beta}^{\mu\nu} \right\rangle \varepsilon_{\mu\nu} - \delta^3 \left\langle z b_{\alpha\beta}^{(1)\mu\nu} \right\rangle u_{3,x_\mu x_\nu}^{(0)} +$$
$$+ \delta^2 \left\langle z b_\mu^{\alpha\beta} \right\rangle \varphi_{x_\mu}^\star + \delta^2 \left\langle z a_\mu^{\alpha\beta} \right\rangle \psi_{x_\mu}^\star + \delta^3 \left\langle z b_{\alpha\beta} \right\rangle T_1^{(0)} +$$
$$+ \delta^3 \left\langle z b_{\alpha\beta}^{(1)} \right\rangle T_2^{(0)}$$

(2.3b)

Likewise, the averaged electric displacement and magnetic induction, see Hadjiloizi et al. [64], are given by:

$$\langle D_\alpha \rangle = \delta \left\langle \delta_\alpha^{\mu\nu} \right\rangle \varepsilon_{\mu\nu} - \delta^2 \left\langle \delta_\alpha^{(1)\mu\nu} \right\rangle u_{3,x_\mu x_\nu}^{(0)} +$$
$$+ \delta \left\langle \delta_{\alpha\mu} \right\rangle \varphi_{x_\mu}^\star + \delta \left\langle \xi_{\alpha\mu} \right\rangle \psi_{x_\mu}^\star + \delta^2 \left\langle \tau_\alpha \right\rangle T_1^{(0)} +$$
$$+ \delta^2 \left\langle \tau_\alpha^{(1)} \right\rangle T_2^{(0)}$$

(2.3c)

$$\langle B_\alpha \rangle = \delta \left\langle \eta_\alpha^{\mu\nu} \right\rangle \varepsilon_{\mu\nu} - \delta^2 \left\langle a_\alpha^{(1)\mu\nu} \right\rangle u_{3,x_\mu \partial x_\nu}^{(0)} +$$
$$+ \delta \left\langle a_{\alpha\mu} \right\rangle \gamma_{x_\mu}^\star + \delta \left\langle \gamma_{\alpha\mu} \right\rangle \omega_{x_\mu} + \delta \left\langle \gamma_\alpha \right\rangle T_1^{(0)} +$$
$$+ \delta \left\langle \gamma_\alpha^{(1)} \right\rangle T_1^{(0)}$$

(2.3d)

Finally, the expressions for the mechanical displacement and the electric and magnetic potentials can be written down as:

$$u_\beta = \left\{ v_\beta - x_3 u_{3,\beta x}^{(0)} \right\} + \delta N_\beta^{\mu\nu} \varepsilon_{\mu\nu} - \delta^2 N_\beta^{(1)\mu\nu} u_{3,x_\mu x_\nu}^{(0)} +$$
$$+ \delta M_\mu^\beta \varphi_{\mu x}^\star + \delta N_\mu^\beta \psi_{\mu x}^\star + \delta^2 G_\beta T_1^{(0)} + \delta^2 G_\beta^{(1)} T_2^{(0)} +$$
$$+ \delta^2 \omega_\beta^\star$$

(2.3e)

$$u_3 = \left\{ u_3^{(0)} + v_3 \right\} + \delta N_3^{\mu\nu} \varepsilon_{\mu\nu} - \delta^2 N_3^{(1)\mu\nu} u_{3,x_\mu x_\nu}^{(0)} +$$
$$+ \delta M_\mu^3 \varphi_{x_\mu}^\star + \delta N_\mu^3 \psi_{x_\mu}^\star + \delta^2 G_3 T_1^{(0)} + \delta^2 G_3^{(1)} T_2^{(0)} +$$
$$+ \delta^2 \omega_3^\star$$

(2.3f)

$$\varphi = \delta \varphi^\star + \delta A_{\mu\alpha} \varepsilon_{\mu\alpha} - \delta^2 A_{\alpha\beta}^{(1)} \hat{u}_{3,x_\alpha x_\beta}^{(0)} + \delta \Xi_\alpha \varphi_{x_\alpha}^\star +$$
$$+ \delta O_\alpha \psi_{x_\alpha}^\star + \delta^2 \Pi T_1^{(0)} + \delta^2 \Pi^{(1)} T_2^{(0)} + \delta^2 \gamma^\star$$

(2.3g)

$$\psi = \delta \psi^\star + \delta \Lambda_{\mu\alpha} \varepsilon_{\mu\alpha} - \delta^2 \Lambda_{\alpha\beta}^{(1)} \hat{u}_{3,x_\alpha x_\beta}^{(0)} + \delta Z_\alpha \varphi_{x_\alpha}^\star +$$
$$+ \delta \Gamma_\alpha \psi_{x_\alpha}^\star + \delta^2 \Delta T_1^{(0)} + \delta^2 \Delta^{(1)} T_2^{(0)} + \delta^2 \omega^\star$$

(2.3h)

Here, $\delta \left\langle b_{\alpha\beta}^{\mu\nu} \right\rangle$, $\delta^2 \left\langle b_{\alpha\beta}^{(1)\mu\nu} \right\rangle$, $\delta \langle \gamma_{\alpha\mu} \rangle$, etc. are the effective coefficients to be determined from the following set of eighteen unit cell problems, see Hadjiloizi et al. [64]:

$$h_\beta^{-1} b_{i\beta,\beta y}^{\mu\alpha} (\mathbf{y}, z) + b_{i3,z}^{\mu\alpha} (\mathbf{y}, z) = 0$$
$$\text{with} \quad b_{ij}^{\mu\alpha} (\mathbf{y}, z) N_j^\pm = 0 \quad \text{on } Z^\pm$$

(2.4a)

$$h_\beta^{-1} b_{\alpha,\beta y}^{i\beta} (\mathbf{y}, z) + b_{\alpha,z}^{i3} (\mathbf{y}, z) = 0$$
$$\text{with} \quad b_\alpha^{ij} (\mathbf{y}, z) N_j^\pm = 0 \quad \text{on } Z^\pm$$

(2.4b)

$$h_\beta^{-1} a_{\alpha,\beta y}^{i\beta} (\mathbf{y}, z) + a_{\alpha,z}^{i3} (\mathbf{y}, z) = 0$$
$$\text{with} \quad a_\alpha^{ij} (\mathbf{y}, z) N_j^\pm = 0 \quad \text{on } Z^\pm$$

(2.4c)

$$h_\beta^{-1} b_{i\beta,\beta y} (\mathbf{y}, z) + b_{i3,z} (\mathbf{y}, z) = 0$$
$$\text{with} \quad b_{ij} (\mathbf{y}, z) N_j^\pm = 0 \quad \text{on } Z^\pm$$

(2.4d)

$$h_\beta^{-1} b_{i\beta,\beta y}^{(1)} (\mathbf{y}, z) + b_{i3,z}^{(1)} (\mathbf{y}, z) = 0$$
$$\text{with} \quad b_{ij}^{(1)} (\mathbf{y}, z) N_j^\pm = 0 \quad \text{on } Z^\pm$$

(2.4e)

$$h_\beta^{-1} b_{i\beta,\beta y}^{(1)\mu\alpha} (\mathbf{y}, z) + b_{i3,z}^{(1)\mu\alpha} (\mathbf{y}, z) = 0$$
$$\text{with} \quad b_{ij}^{\mu\alpha} (\mathbf{y}, z) N_j^\pm = 0 \quad \text{on } Z^\pm$$

(2.4f)

$$h_\beta^{-1} \eta_{\beta,\beta y}^{i\alpha} (\mathbf{y}, z) + \eta_{3,z}^{i\alpha} (\mathbf{y}, z) = 0$$
$$\text{with} \quad \eta_j^{i\alpha} (\mathbf{y}, z) N_j^\pm = 0 \quad \text{on } Z^\pm$$

(2.5a)

$$h_\beta^{-1} a_{\beta\alpha,\beta y} (\mathbf{y}, z) + a_{3\alpha,z} (\mathbf{y}, z) = 0$$
$$\text{with} \quad a_{j\alpha} (\mathbf{y}, z) N_j^\pm = 0 \quad \text{on } Z^\pm$$

(2.5b)

$$h_\beta^{-1} \gamma_{\beta\alpha,\beta y} (\mathbf{y}, z) + \gamma_{3\alpha,z} (\mathbf{y}, z) = 0$$
$$\text{with} \quad \gamma_{j\alpha} (\mathbf{y}, z) N_j^\pm = 0 \quad \text{on } Z^\pm$$

(2.5c)

$$h_\beta^{-1} \gamma_{\beta,\beta y} (\mathbf{y}, z) + \gamma_{3,z} (\mathbf{y}, z) = 0$$
$$\text{with} \quad \gamma_j (\mathbf{y}, z) N_j^\pm = 0 \quad \text{on } Z^\pm$$

(2.5d)

$$h_\beta^{-1}\gamma_{\beta,\beta y}^{(1)}(\mathbf{y},z)+\gamma_{3,z}^{(1)}(\mathbf{y},z)=0$$
$$\text{with}\quad \gamma_j^{(1)}(\mathbf{y},z)\,N_j^\pm=0\quad\text{on }Z^\pm \tag{2.5e}$$

$$h_\beta^{-1}a_{\beta,\beta y}^{(1)\mu\alpha}(\mathbf{y},z)+a_{3,z}^{(1)\mu\alpha}(\mathbf{y},z)=0$$
$$\text{with}\quad a_i^{\mu\alpha}(\mathbf{y},z)\,N_j^\pm=0\quad\text{on }Z^\pm \tag{2.5f}$$

$$h_\beta^{-1}\delta_{\beta,\beta y}^{i\alpha}(\mathbf{y},z)+\delta_{3,z}^{i\alpha}(\mathbf{y},z)=0$$
$$\text{with}\quad \delta_j^{i\alpha}(\mathbf{y},z)\,N_j^\pm=0\quad\text{on }Z^\pm \tag{2.6a}$$

$$h_\beta^{-1}\delta_{\beta\alpha,\beta y}(\mathbf{y},z)+\delta_{3\alpha,z}(\mathbf{y},z)=0$$
$$\text{with}\quad \delta_{j\alpha}(\mathbf{y},z)\,N_j^\pm=0\quad\text{on }Z^\pm \tag{2.6b}$$

$$h_\beta^{-1}\xi_{\beta\alpha,\beta y}(\mathbf{y},z)+\xi_{3\alpha,z}(\mathbf{y},z)=0$$
$$\text{with}\quad \xi_{j\alpha}(\mathbf{y},z)\,N_j^\pm=0\quad\text{on }Z^\pm \tag{2.6c}$$

$$h_\beta^{-1}\tau_{\beta,\beta y}(\mathbf{y},z)+\tau_{3,z}(\mathbf{y},z)=0$$
$$\text{with}\quad \tau_j(\mathbf{y},z)\,N_j^\pm=0\quad\text{on }Z^\pm \tag{2.6d}$$

$$h_\beta^{-1}\tau_{\beta,\beta y}^{(1)}(\mathbf{y},z)+\tau_{3,z}^{(1)}(\mathbf{y},z)=0$$
$$\text{with}\quad \tau_j^{(1)}(\mathbf{y},z)\,N_j^\pm=0\quad\text{on }Z^\pm \tag{2.6e}$$

$$h_\beta^{-1}\delta_{\beta,\beta y}^{(1)\mu\alpha}(\mathbf{y},z)+\delta_{3,z}^{(1)\mu\alpha}(\mathbf{y},z)=0$$
$$\text{with}\quad \delta_i^{\mu\alpha}(\mathbf{y},z)\,N_j^\pm=0\quad\text{on }Z^\pm \tag{2.6f}$$

where,

$$b_{ij}^{k\alpha}=L_{ijm}N_m^{k\alpha}+M_{ij}A_{k\alpha}+N_{ij}\Lambda_{k\alpha}+C_{ijk\alpha},$$
$$b_\alpha^{ij}=L_{ijm}M_\alpha^m+M_{ij}\Xi_\alpha+N_{ij}Z_\alpha+e_{\alpha ij}$$
$$a_\alpha^{ij}=L_{ijm}N_\alpha^m+M_{ij}O_\alpha+N_{ij}\Gamma_\alpha+Q_{\alpha ij},$$
$$b_{ij}=L_{ijm}G_m+M_{ij}\Pi+N_{ij}\Delta-\Theta_{ij} \tag{2.7a}$$
$$b_{ij}^{(1)}=L_{ijm}G_m^{(1)}+M_{ij}\Pi^{(1)}+N_{ij}\Delta^{(1)}-z\Theta_{ij},$$
$$b_{ij}^{(1)k\alpha}=L_{ijm}N_m^{(1)k\alpha}+M_{ij}A_{k\alpha}^{(1)}+N_{ij}\Lambda_{k\alpha}^{(1)}+zC_{ijk\alpha}$$

$$\eta_j^{k\alpha}=L_{ji}N_i^{k\alpha}-M_jA_{k\alpha}-N_j(y)\Lambda_{k\alpha}+Q_{jk\alpha},$$
$$a_{j\alpha}=L_{ji}M_\alpha^i-M_j\Xi_\alpha-N_jZ_\alpha-\lambda_{j\alpha}$$
$$\gamma_{j\alpha}=L_{ji}N_\alpha^i-M_jO_\alpha-N_j\Gamma_\alpha-\mu_{j\alpha},$$
$$\gamma_j=L_{ji}G_i-M_j\Pi-N_j\Delta-\eta_j, \tag{2.7b}$$
$$\gamma_j^{(1)}=L_{ji}G_i^{(1)}-M_j\Pi^{(1)}-N_j\Delta^{(1)}+z\eta_j,$$
$$a_i^{(1)k\alpha}=L_{im}N_m^{(1)k\alpha}-M_iA_{k\alpha}^{(1)}-N_i\Lambda_{k\alpha}^{(1)}+zQ_{ik\alpha}$$

$$\delta_j^{k\alpha}=L_{ji}^\star N_i^{k\alpha}-M_j^\star A_{k\alpha}-N_j^\star \Lambda_{k\alpha}+e_{jk\alpha},$$
$$\delta_{j\alpha}=L_{ji}^\star M_\alpha^i-M_j^\star\Xi_\alpha-N_j^\star Z_\alpha-\varepsilon_{j\alpha}$$
$$\xi_{j\alpha}=L_{ji}^\star N_\alpha^i-M_j^\star O_\alpha-N_j^\star\Gamma_\alpha-\lambda_{j\alpha}, \tag{2.7c}$$
$$\tau_j=L_{ji}^\star G_i-M_j^\star\Pi-N_j^\star\Delta+\xi_j,$$
$$\tau_j^{(1)}=L_{ji}^\star G_i^{(1)}-M_j^\star\Pi^{(1)}-N_j^\star\Delta^{(1)}+z\xi_j,$$
$$\delta_i^{(1)k\alpha}=L_{im}^\star N_m^{(1)k\alpha}-M_i^\star A_{k\alpha}^{(1)}-N_i^\star\Lambda_{k\alpha}^{(1)}+ze_{ik\alpha}$$

and $N_m^{k\alpha}$, $A_{k\alpha}$, $\Lambda_{k\alpha}$, etc. are local functions, which define the asymptotic expansions of the mechanical displacement and electric and magnetic potentials, respectively, see Eqs. 2.3e – 2.3h. Furthermore, L_{ijm}, M_{ij}, N_{ij} etc. are differential operators defined in Eqs. (I-6.2a), (I-6.4a) and

(I-6.6a). Note that in the previous sentence and from this point onwards, for the sake of convenience, all equations that are referenced from Hadjiloizi et al. [64] will be denoted by the uppercase letter I preceding the corresponding equation number. For example, Eq. (I-5.27a) will denote Eq. 5.27a in Hadjiloizi et al. [64].

3 Applications of the General Model – Constant Thickness Laminates

We will illustrate our work by means of several examples. The first examples are for laminates of constant thickness, as shown in Fig. 1. As shown in the unit cell of Fig. 1, each layer is completely determined by the parameters δ_1, $\delta_2,\ldots\delta_M$ where M is the total number of layers. The thickness of the mth layer is therefore δ_m-δ_{m-1} with $\delta_0=0$ and $\delta_M=1$. The real thickness of the mth layer as measured in the original (x_1,x_2,x_3) coordinate system is $\delta(\delta_m-\delta_{m-1})$, where δ is the thickness of the laminate (again with respect to the original coordinate system).
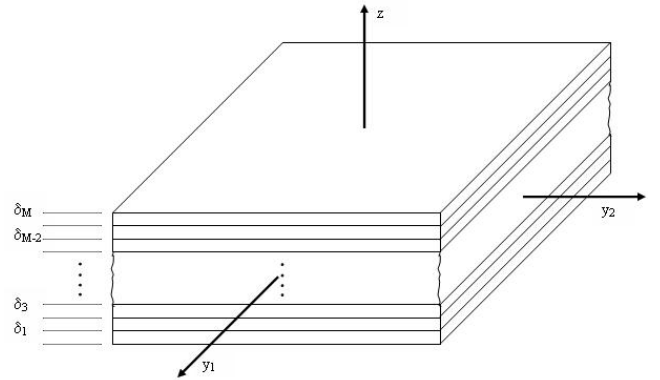

Figure 1: Unit cell of a laminated magnetoelectric composite plate.

It is apparent that all material parameters are independent of y_1 and y_2, and consequently, all partial derivatives in Eqs. 2.4a- 2.7c become ordinary derivatives with respect to z. We will consider laminates made up of perfectly bonded laminae of piezoelectric and piezomagnetic materials with the poling and magnetization directions along the z-axis. The "perfect bonding" assumption is akin to neglecting the interphase layers between adjacent plies. (Because the interphase regions might be important in the case of nano-laminates, application of the derived models to such structures might need to take the interphase lay-

ers into consideration, see for example Sevostianov and Kachanov for particulate-reinforced nanocomposites [65]). Furthermore, the overall thickness of the laminate is considered to be small compared to the in-plane dimensions. For the sake of generality, we will also assume that the constituent materials are made of orthotropic materials, with the principal material coordinate axes not necessarily coinciding with the y_1, y_2, z system but with a system that has been rotated by an arbitrary angle with respect to the z axis. As such, the pertinent coefficient matrices (tensors) are the same as those of a monoclinic material, as far as the number and location of the non-zero coefficients is concerned, see Reddy [68]. Thus:

$$
\begin{bmatrix}
C_{11} & C_{12} & C_{13} & 0 & 0 & C_{16} \\
C_{12} & C_{22} & C_{23} & 0 & 0 & C_{26} \\
C_{13} & C_{23} & C_{33} & 0 & 0 & C_{36} \\
0 & 0 & 0 & C_{44} & C_{45} & 0 \\
0 & 0 & 0 & C_{45} & C_{55} & 0 \\
C_{16} & C_{26} & C_{36} & 0 & 0 & C_{66}
\end{bmatrix}
$$

$$
\begin{bmatrix}
0 & 0 & e_{31} \\
0 & 0 & e_{32} \\
0 & 0 & e_{33} \\
e_{14} & e_{24} & 0 \\
e_{15} & e_{25} & 0 \\
0 & 0 & 0
\end{bmatrix}^T
\quad
\begin{bmatrix}
\Theta_{11} & \Theta_{12} & 0 \\
\Theta_{12} & \Theta_{22} & 0 \\
0 & 0 & \Theta_{33}
\end{bmatrix}
\quad
\begin{bmatrix}
\xi_1 \\
\xi_2 \\
\xi_3
\end{bmatrix}
$$

(3.1)

In Eq. 3.1 the first matrix is the elasticity tensor, the second matrix represents the tensor of piezoelectric or piezomagnetic coefficients, the third matrix pertains to the thermal expansion (or dielectric permittivity/magnetic permeability/magnetoelectric) tensor, and the last vector is the pyroelectric or pyromagnetic tensor. We will now proceed with the solution of the unit cell problems and the determination of general expressions for the effective coefficients.

(a) Unit Cell Problems 2.4a, 2.5a and 2.6a

To obtain the effective properties, the following procedure will be adhered to: The unit cell problems 2.4a-2.6f will be reduced to ordinary differential equations in z due to the aforementioned independency on y_1 and y_2. The pertinent boundary conditions will also be simplified, because the normal vector N becomes (0,0,1). Subsequently, the reduced unit cell problems will be solved in a straight-forward manner, giving the coefficient functions $b_{ij}^{k\alpha}$, $\eta_j^{\mu\nu}$, $\delta_j^{k\alpha}$ etc. as defined in Eqs. 2.7a – 2.7c. Because each of these functions is in turn a function of three local functions (for example Eq. 2.7a shows that $b_{ij}^{k\alpha}$ is a function of $N_m^{k\alpha}$, $A_{k\alpha}$, and $\Lambda_{k\alpha}$), we will need a total of three unit cell problems to solve for the three unknowns. Hence, we will look for the three unit cell problems that use

these same local functions. For example, local functions $N_m^{k\alpha}$, $A_{k\alpha}$, and $\Lambda_{k\alpha}$ appear in unit cell problems 2.4a, 2.5a and 2.6a via coefficient functions $b_{ij}^{k\alpha}$, $\eta_j^{\mu\nu}$ and $\delta_j^{k\alpha}$. Finally, after obtaining these local functions, we will back-substitute them into the appropriate expressions for the coefficient functions which in turn yield the effective coefficients after applying the homogenization procedure of Eq. (I-4.5a).

Based on the above procedure, Eq. 2.4a reduces to:

$$\frac{db_{i3}^{k\alpha}(z)}{dz} = 0 \quad \text{with} \quad b_{i3}^{k\alpha}(z) = 0 \quad \text{on } Z^\pm \quad (3.2a)$$

Solving 3.2a leads to $b_{i3}^{k\alpha} = 0$ everywhere in the unit cell. From Eq. (I-5.2a) and the first expression in Eq. 2.7a we have:

$$b_{i3}^{\mu\alpha} = C_{i3n3}\frac{dN_n^{\mu\alpha}}{dz} + e_{3i3}\frac{dA_{\mu\alpha}}{dz} + Q_{3i3}\frac{d\Lambda_{\mu\alpha}}{dz} + C_{i3\mu\alpha} = 0 \quad (3.2b)$$

Letting i = 1, 2 in Eq. 3.2b and bearing in mind the orthotropy of the constituents, see Eq. 3.1, we readily see that:

$$\frac{\partial N_1^{\mu\alpha}}{\partial z} = \frac{\partial N_2^{\mu\alpha}}{\partial z} = 0 \quad (3.2c)$$

For i = 3, Eq. 3.2b yields:

$$C_{33}\frac{dN_3^{\mu\alpha}}{dz} + e_{33}\frac{dA_{\mu\alpha}}{dz} + Q_{33}\frac{d\Lambda_{\mu\alpha}}{dz} = -C_{33\mu\alpha} \quad (3.2d)$$

Eq. 3.2d contains three unknown functions, $\frac{dN_3^{\mu\alpha}}{dz}$, $\frac{dA_{\mu\alpha}}{dz}$, $\frac{d\Lambda_{\mu\alpha}}{dz}$. Hence, we will need two more equations which will come from unit-cell problems 2.5a and 2.6a. Following the same procedure as above, and keeping Eq. 3.2c in mind, these unit-cell problems yield the following equations:

$$Q_{33}\frac{dN_3^{\mu\alpha}}{dz} - \lambda_{33}\frac{dA_{\mu\alpha}}{dz} - \mu_{33}\frac{d\Lambda_{\mu\alpha}}{dz} = -Q_{3\mu\alpha}$$

(3.2e)

$$e_{33}\frac{dN_3^{\mu\alpha}}{dz} - \varepsilon_{33}\frac{dA_{\mu\alpha}}{dz} - \lambda_{33}\frac{d\Lambda_{\mu\alpha}}{dz} = -e_{3\mu\alpha}$$

Solving Eqs. 3.2d and 3.2e as a system yields the following solution:

$$\frac{dN_3^{\mu\alpha}}{dz} = \frac{(e_{3\mu\alpha}\lambda_{33} - Q_{3\mu\alpha}\varepsilon_{33})Q_{33}}{\hat{\Pi}_1} +$$
$$+ \frac{\lambda_{33}^2 C_{33\mu\alpha} + \lambda_{33}e_{33}Q_{3\mu\alpha} - \mu_{33}e_{33}e_{3\mu\alpha} - \mu_{33}\varepsilon_{33}C_{33\mu\alpha}}{\hat{\Pi}_1}$$

(3.2f)

$$\frac{dA_{\mu\alpha}}{dz} = \frac{(Q_{3\mu\alpha}e_{33} + C_{33\mu\alpha}\lambda_{33})Q_{33} + Q_{33}^2 e_{3\mu\alpha}}{\hat{\Pi}_1} +$$
$$+ \frac{-\lambda_{33}C_{33}Q_{3\mu\alpha} - \mu_{33}e_{33}C_{33\mu\alpha} + \mu_{33}C_{33}e_{3\mu\alpha}}{\hat{\Pi}_1}$$

(3.2g)

$$\frac{d\Lambda_{\mu\alpha}}{dz}=\frac{\left(-e_{3\mu\alpha}e_{33}-C_{33\mu\alpha}\varepsilon_{33}\right)Q_{33}+e_{33}^2 Q_{3\mu\alpha}}{\hat{\Pi}_1}+$$
$$+\frac{\varepsilon_{33}C_{33}Q_{3\mu\alpha}+\lambda_{33}e_{33}C_{33\mu\alpha}-\lambda_{33}C_{33}e_{3\mu\alpha}}{\hat{\Pi}_1}$$
(3.2h)

where $\hat{\Pi}_1=\mu_{33}C_{33}\varepsilon_{33}-C_{33}\lambda_{33}^2+Q_{33}^2\varepsilon_{33}+$
$-2\lambda_{33}Q_{33}e_{33}+\mu_{33}e_{33}^2$
(3.2i)

Using these solutions, the in-plane elastic, piezoelectric and piezomagnetic functions (from which the effective coefficients will be computed in the sequel) may be calculated as follows:

$$b_{\alpha\beta}^{\mu\nu}=C_{\alpha\beta33}\frac{dN_3^{\mu\nu}}{dz}+e_{3\alpha\beta}\frac{d\Lambda_{\mu\nu}}{dz}+Q_{3\alpha\beta}\frac{dA_{\mu\nu}}{dz}+C_{\alpha\beta\mu\nu}$$
[In – plane elastic functions]

(3.3a)

$$\eta_{\beta}^{\mu\nu}=0 \quad \text{[In – plane piezoelectric functions]}$$ (3.3b)

$$\delta_{\beta}^{\mu\nu}=0 \text{ [In – plane piezomagnetic functions]}$$ (3.3c)

Two features are worth mentioning here. First of all, it can be seen that the elastic functions (and as a consequence the effective extensional elastic coefficients) depend not only on the elastic parameters of the constituent phases, but also on the piezoelectric, piezomagnetic, and magnetoelectric coefficients, as well as the dielectric permittivities and magnetic permeabilities. This is in marked contrast with previous simpler models, see Kalamkarov and Georgiades [60], which predicted that the extensional elastic coefficients depend only on the elastic parameters of the constituents. Therefore, the present work constitutes an important refinement over previously established results. Also, for the case of simple laminates such as the ones considered in this section, the work presented here represents an extension of the classical composite laminate theory (see e.g. [66], [67]) to piezo-magneto-thermo-elastic structures. Of course, if piezoelectric and piezomagnetic effects are completely ignored, then Eq. 3.3a reduces to:

$$b_{\alpha\beta}^{\mu\nu}=-C_{\alpha\beta33}\frac{C_{33\mu\nu}}{C_{33}}+C_{\alpha\beta\mu\nu}$$ (3.3d)

which conforms exactly to the results of Kalamkarov and Georgiades [60], Georgiades and Kalamkarov [61] as well as the classical composite laminate theory. The second feature that is evident in Eqs. 3.3b and 3.3c is that the in-plane piezoelectric and piezomagnetic functions are zero. Clearly, this is because of the fact that the polarization/magnetization directions are the same as the stacking orientation. Had we chosen polarization and magnetization directions along y_1 or y_2 the results would be drastically different. Herein lies a significant advantage of our model: it can be tailored to meet the specific requirements of an engineering application by changing one or more geometric, physical or material parameters.

(b) Unit Cell Problems 2.4b, 2.5b and 2.6b

Eq. 2.4b reduces to:

$$\frac{db_{\alpha}^{i3}(z)}{dz}=0$$
with $b_{\alpha}^{i3}(z)=0$ on $Z^{\pm}$
(3.4a)

Solving 3.4a leads to $b_{\alpha}^{i3}=0$ everywhere in the unit cell. From the second expression in Eq. 2.7a and Eq. (I-5.2a) we have:

$$b_{\alpha}^{i3}=C_{i3n3}\frac{dM_{\alpha}^n}{dz}+e_{3i3}\frac{d\Xi_{\alpha}}{dz}+Q_{3i3}\frac{dZ_{\alpha}}{dz}+e_{\alpha i3}=0$$ (3.5a)

Letting n =1, 2 in Eq. 3.5a while keeping Eq. 3.1 in mind, leads to two simultaneous equations in $\frac{dM_{\alpha}^1}{dz}$ and $\frac{dM_{\alpha}^2}{dz}$. Their solution is readily found to be:

$$\frac{dM_{\alpha}^1}{dz}=\frac{C_{45}e_{\alpha23}-C_{44}e_{\alpha13}}{C_{44}C_{55}-C_{45}^2}, \quad \frac{dM_{\alpha}^2}{dz}=\frac{C_{45}e_{\alpha13}-C_{55}e_{\alpha23}}{C_{44}C_{55}-C_{45}^2}$$
(3.5b)

Letting n = 3 in Eq. 3.5a leads to a homogeneous equation in three unknown functions:

$$C_{33}\frac{dM_{\alpha}^3}{dz}+e_{33}\frac{dZ_{\alpha}}{dz}+Q_{33}\frac{d\Xi_{\alpha}}{dz}=0$$ (3.5c)

As we need two more equations, we resort to unit cell problems 2.5b and 2.6b. Following the same procedure as above we end up with:

$$Q_{33}\frac{dM_{\alpha}^3}{dz}-\mu_{33}\frac{dZ_{\alpha}}{dz}-\lambda_{33}\frac{d\Xi_{\alpha}}{dz}=0$$
$$e_{33}\frac{dM_{\alpha}^3}{dz}-\lambda_{33}\frac{dZ_{\alpha}}{dz}-\varepsilon_{33}\frac{d\Xi_{\alpha}}{dz}=0$$
(3.5d)

The solution of Eqs. 3.5c and 3.5d gives:

$$\frac{dM_{\alpha}^3}{dz}=\frac{dZ_{\alpha}}{dz}=\frac{d\Xi_{\alpha}}{dz}=0$$ (3.5e)

Using Eqs. 3.5b and 3.5e we obtain the in-plane piezoelectric, magnetoelectric and dielectric permittivity functions from which their effective coefficient counterparts may easily be determined (as will be shown shortly):

$$-a_{\mu\alpha}=Q_{\mu13}\frac{C_{44}e_{\alpha13}-C_{45}e_{\alpha23}}{C_{44}C_{55}-C_{45}^2}+Q_{\mu23}\frac{C_{55}e_{\alpha23}-C_{45}e_{\alpha13}}{C_{44}C_{55}-C_{45}^2}+\lambda_{\mu\alpha}$$
[Magnetoelectric functions]

(3.6a)

$$-\delta_{\mu\alpha}=e_{\mu13}\frac{C_{44}e_{\alpha13}-C_{45}e_{\alpha23}}{C_{44}C_{55}-C_{45}^2}+e_{\mu23}\frac{C_{55}e_{\alpha23}-C_{45}e_{\alpha13}}{C_{44}C_{55}-C_{45}^2}+\varepsilon_{\mu\alpha}$$
[Dielectric permittivity]

(3.6b)

$$b_\alpha^{\mu\nu} = 0 \text{ [In – plane piezoelectric } functions]} \qquad (3.6c)$$

The reason why the in-plane piezoelectric functions vanish was explained above. Also, we note the appearance of the magnetoelectric functions (first product properties).

(c) Unit Cell Problems 2.4c, 2.5c and 2.6c

Similarly to the previous three unit cell problems, Eqs. 2.4c, 2.5c and 2.6c are easily solved, yielding:

$$\frac{dN_\alpha^1}{dz} = \frac{C_{45}Q_{\alpha 23} - C_{44}Q_{\alpha 13}}{C_{44}C_{55} - C_{45}^2}, \qquad \frac{dN_\alpha^2}{dz} = \frac{C_{45}Q_{\alpha 13} - C_{55}Q_{\alpha 23}}{C_{44}C_{55} - C_{45}^2},$$
$$\frac{dN_\alpha^3}{dz} = \frac{dO_\alpha}{dz} = \frac{d\Gamma_\alpha}{dz} = 0$$
$$(3.7a)$$

Using these results, the in-plane piezomagnetic, magnetic permeability and magnetoelectric functions are derived as follows:

$$-\gamma_{\mu\alpha} = Q_{\mu 13}\frac{C_{44}Q_{\alpha 13} - C_{45}Q_{\alpha 23}}{C_{44}C_{55} - C_{45}^2} + Q_{\mu 23}\frac{C_{55}Q_{\alpha 23} - C_{45}Q_{\alpha 13}}{C_{44}C_{55} - C_{45}^2} + \mu_{\mu\alpha}$$
[Magnetic permeability]
$$(3.7b)$$

$$-\xi_{\mu\alpha} = e_{\mu 13}\frac{C_{44}Q_{\alpha 13} - C_{45}Q_{\alpha 23}}{C_{44}C_{55} - C_{45}^2} + e_{\mu 23}\frac{C_{55}Q_{\alpha 23} - C_{45}Q_{\alpha 13}}{C_{44}C_{55} - C_{45}^2} + \lambda_{\mu\alpha}$$
[Magnetoelectric functions]
$$(3.7c)$$

$$a_\alpha^{\mu\nu} = 0 \text{ [Piezomagnetic functions]} \qquad (3.7d)$$

(d) Unit Cell Problems 2.4d, 2.5d and 2.6d

Proceeding as above, we arrive at the following results:

$$\frac{dG_3}{dz} = \frac{\lambda_{33}Q_{33}\xi_3 - Q_{33}\varepsilon_{33}\eta_3 - \lambda_{33}^2\Theta_{33}}{\hat{\Pi}_1} + \\ + \frac{\lambda_{33}e_{33}\eta_3 - \mu_{33}e_{33}\xi_3 + `\mu_{33}\Theta_{33}\varepsilon_{33}}{\hat{\Pi}_1} \qquad (3.8a)$$

$$\frac{d\Delta}{dz} = \frac{-\xi_3 e_{33}Q_{33} + \Theta_{33}\varepsilon_{33}Q_{33} + e_{33}^2\eta_3}{\hat{\Pi}_1} + \\ + \frac{\varepsilon_{33}C_{33}\eta_3 - \lambda_{33}e_{33}\Theta_{33} - \lambda_{33}C_{33}\xi_3}{\hat{\Pi}_1} \qquad (3.8b)$$

$$\frac{d\Pi}{dz} = \frac{-Q_{33}e_{33}\eta_3 - \Theta_{33}\lambda_{33}Q_{33} + Q_{33}^2\xi_3}{\hat{\Pi}_1} + \\ + \frac{-\lambda_{33}C_{33}\eta_3 + \mu_{33}\Theta_{33}e_{33} + \mu_{33}C_{33}\xi_3}{\hat{\Pi}_1} \qquad (3.8c)$$

$$\frac{\partial G_1}{\partial z} = \frac{\partial G_2}{\partial z} = 0 \qquad (3.8d)$$

With these results we can calculate the thermal expansion, pyroelectric and pyromagnetic functions related to the mid-plane temperature variation. We recall from Eq. (I-3.4b), that (as is customary in heat conduction studies of thin plates and shells) we assume a temperature variation that is the superposition of a mid-plane term and a linear through-the-thickness term. The set of coefficients stemming from Eqs. 3.8a- 3.8d is related to the mid-plane term. Thus:

$$-b_{\alpha\beta} = -C_{\alpha\beta 33}\frac{dG_3}{dz} - e_{3\alpha\beta}\frac{d\Pi}{dz} - Q_{3\alpha\beta}\frac{d\Delta}{dz} + \Theta_{\alpha\beta}$$
[In – plane thermal expansion functions]
$$(3.9a)$$

$$\gamma_\alpha = \eta_\alpha \quad \text{[In – plane pyromagnetic functions]} \qquad (3.9b)$$

$$\tau_\alpha = \xi_\alpha \quad \text{[In – plane pyroelectric functions]} \qquad (3.9c)$$

(e) Unit Cell Problems 2.4e, 2.5e and 2.6e

Following the above procedure it can be seen that:

$$\frac{dG_3^{(1)}}{dz} = z\frac{dG_3}{dz}, \qquad \frac{d\Pi^{(1)}}{dz} = z\frac{d\Pi}{dz}, \qquad \frac{d\Delta^{(1)}}{dz} = z\frac{d\Delta}{dz} \quad (3.10a)$$

Hence, the solution of the secondary pyroelectric and pyromagnetic as well as in-plane thermal expansion functions (all related to the through-the-thickness temperature variation) is given simply by:

$$b_{\alpha\beta}^{(1)} = zb_{\alpha\beta}, \qquad \gamma_\alpha^{(1)} = z\gamma_\alpha, \qquad \tau_\alpha^{(1)} = z\tau_\alpha \qquad (3.10b)$$

(f) Unit Cell Problems 2.4f, 2.5f and 2.6f

Similarly, solving these three unit-cell problems yields:

$$b_{\alpha\beta}^{(1)\mu\nu} = zb_{\alpha\beta}^{\mu\nu} \text{ [Elastic coupling functions]} \qquad (3.11a)$$

$$a_\alpha^{(1)\mu\nu} = zb_\alpha^{\mu\nu} = 0$$
[Out – of – plane piezoelectric functions]
$$(3.11b)$$

$$\delta_\alpha^{(1)\mu\nu} = z\delta_\alpha^{\mu\nu} = 0$$
[Out – of – plane piezomagnetic functions]
$$(3.11c)$$

The last set of functions that we need to consider are the elastic bending functions shown in Eq. (I-6.2b). It is evident that:

$$zb_{\alpha\beta}^{(1)\mu\nu} = z^2 b_{\alpha\beta}^{\mu\nu} \text{ [Elastic bending functions]} \qquad (3.11d)$$

(g) Effective Coefficients and Numerical Examples

The effective coefficients are obtained in a straightforward fashion by directly applying the homogenization procedure in Eq. (I-4.5a). For example, referring to Fig. 1, one can see that the extensional effective elastic coefficients are given by:

$$
\left\langle b_{\alpha\beta}^{\lambda\mu} \right\rangle = \int_{-0.5}^{0.5} b_{\alpha\beta}^{\lambda\mu} dz = \int_{0}^{1} b_{\alpha\beta}^{\lambda\mu} d\delta_m =
$$
$$
= \sum_{m=1}^{M} \int_{\delta_{m-1}}^{\delta_m} b_{\alpha\beta}^{\lambda\mu} d\delta_m = b_{\alpha\beta}^{\lambda\mu(m)} (\delta_m - \delta_{m-1})
$$

(3.12a)

Likewise, the coupling and bending effective elastic coefficients are given by:

$$
\left\langle zb_{\alpha\beta}^{\lambda\mu} \right\rangle = \left\langle b_{\alpha\beta}^{(1)\lambda\mu} \right\rangle =
$$
$$
= \frac{1}{2} \sum_{m=1}^{M} b_{\alpha\beta}^{\lambda\mu(m)} \left(\delta_m^2 - \delta_{m-1}^2 - (\delta_m - \delta_{m-1}) \right),
$$
$$
\left\langle zb_{\alpha\beta}^{(1)\lambda\mu} \right\rangle = \left\langle z^2 b_{\alpha\beta}^{\lambda\mu} \right\rangle =
$$
$$
= \frac{1}{3} \sum_{m=1}^{M} b_{\alpha\beta}^{\lambda\mu(m)} \left(\delta_m^3 - \delta_{m-1}^3 + \right.
$$
$$
\left. - \frac{3}{2} \left(\delta_m^2 - \delta_{m-1}^2 \right) + \frac{3}{4} (\delta_m - \delta_{m-1}) \right).
$$

(3.12b)

In the same manner, the remaining effective elastic coefficients may be determined.

We will illustrate our work by considering a simple 4-ply laminate consisting of alternating barium titanate (top layer) and cobalt ferrite laminae. The overall thickness of the laminate is 1 mm. The pertinent material parameters are given in Table 1. For the sake of discussion we will further assume that the Barium Titanate is doped with Fe so that it exhibits primary magnetoelectricity. For illustration purposes only, we will presume that the value of the magnetoelectric coefficient of bulk Fe-doped BaTiO$_3$ is similar to that pertaining to a nanostructured counterpart, and is $\sim$16 mV/Oe cm, see Verma et al. [72]. Thus, in the parlance of our present work (we define the magnetoelectric coefficients slightly differently, see Section 2) and for a dielectric permittivity value of around 11.2×10^{-9}C^2/N m^2 (Table 1) we assume that $\lambda_{11} = \lambda_{22} = \lambda_{33}$ is $\approx 2.2 \times 10^{-10}$ C/A m. We will also assume that the Fe doping does not affect the remaining properties of BaTiO$_3$ as shown in Table 1. Likewise, we will assume that the cobalt ferrite is doped with the rare earth element Dy, see Dascalu et al. [73], so that it too exhibits primary magnetoelectricity. The pertinent magnetoelectric value ≈ -2.5 μV/Oe cm. Thus, for a dielectric permittivity value of around 0.08×10^{-9}C^2/N m^2 (Table 1) we can assume that $\lambda_{11} = \lambda_{22} = \lambda_{33}$ is $\approx 0.25 \times 10^{-15}$ C/A m.

Fig. 2 shows the variation of the $\left\langle zb_{22}^{(1)22} \right\rangle$ bending coefficient vs. the thickness of the BaTiO$_3$ laminae. It can clearly be seen that the effective elastic coefficients change

Table 1: Material properties of BaTiO$_3$, and CoFe$_2$O$_4$ (Li and Dunn [69], Yoshihiro and Tanigawa, [70], Cook et al., [71]).

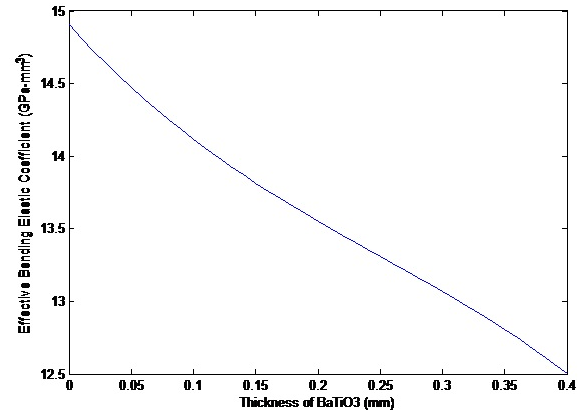|	BaTiO$_3$	CoFe$_2$O$_4$
$C_{11} = C_{22}$ (GPa)	166	286
C_{12} (GPa)	77	173
$C_{13} = C_{23}$ (GPa)	78	170
C_{33} (GPa)	162	269.5
$C_{44} = C_{55}$ (GPa)	43	45.3
$e_{31} = e_{32}$ (C/m^2)	−4.4	0
e_{33} (C/m^2)	18.6	0
$e_{24} = e_{15}$ (C/m^2)	11.6	0
$\varepsilon_{11} = \varepsilon_{22}$ (10^{-9} C^2/N m^2)	11.2	0.08
ε_{33} (10^{-9} C^2/N m^2)	12.6	0.093
$Q_{31} = Q_{32}$ (N/A m)	0	580.3
Q_{33} (N/A m)	0	699.7
$Q_{24} = Q_{15}$ (N/A m)	0	550
$\mu_{11} = \mu_{22}$ (10^{-6} N s^2/C^2)	5	−590
μ_{33} (10^{-6} N s^2/C^2)	10	157
$\alpha_{11} = \alpha_{22}$ (10^{-6} 1/K)	15.7	10
α_{33} (10^{-6} 1/K)	6.4	10
$\xi_1 = \xi_2 = \xi_3$ (10^{-4} C/m^{2}K)	1.5	0

Figure 2: Plot of effective $\left\langle zb_{22}^{(1)22} \right\rangle$ bending coefficient vs. thickness of the BaTiO$_3$ laminae.

significantly as the relative volume fractions of the constituents change. Since cobalt ferrite is generally stiffer than its barium titanate counterpart, increasing the overall thickness of the latter causes a corresponding reduction in the value of the effective bending coefficients.

Fig. 3 shows the variation of the effective $\left\langle zb_{11}^{11} \right\rangle$ coupling coefficient vs. the thickness of the BaTiO$_3$ laminae. As expected, the absence of barium titanate renders the laminate symmetric and nullifies the effective coupling coefficients. As the thickness of this constituent increases,
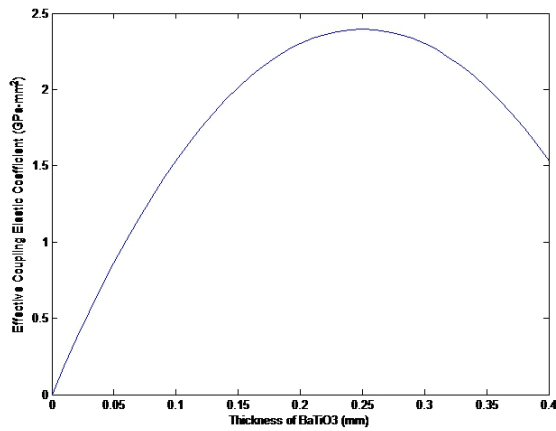
Figure 3: Plot of effective $\langle zb_{11}^{11} \rangle$ coupling coefficient vs. thickness of the BaTiO$_3$ laminae.
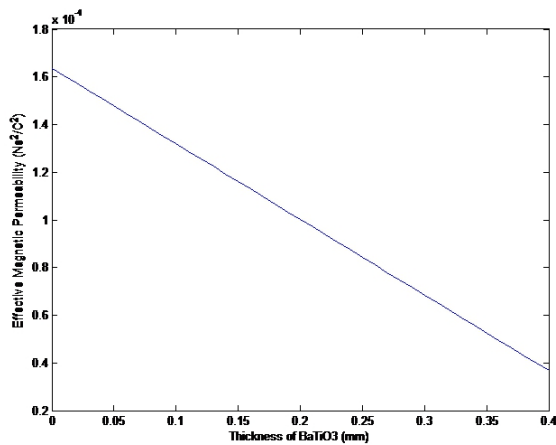

Figure 4: Plot of effective $\langle \gamma_{11} \rangle$ magnetic permeability coefficient vs. thickness of the BaTiO$_3$ laminae.

the laminate becomes more asymmetric, and the effective coupling coefficients increase. Finally, as the thickness of barium titanate approaches 0.5 (which is tantamount to having no cobalt ferrite - the entire structure is made of BaTiO$_3$) the effective coupling coefficients approach zero, as the laminate approaches geometric symmetry with respect to the mid-plane.

Figs. 4 and 5 show the variation of the effective magnetic permeability,$\langle \gamma_{11} \rangle$, and the magnetoelectric product coefficient $\langle \xi_{11} \rangle$. As expected, reducing the volume fraction of Dy-doped CoFe$_2$O$_4$ results in a corresponding reduction of the effective magnetic permeability coefficients and an increase in the effective magnetoelectric coefficients. What is important to emphasize here though, is that these trends may be easily changed, if the polarization and /or magnetization directions for the constituent

materials are altered, if the nature of the doping materials is changed, if the stacking configuration of the laminae is rearranged etc. In essence, our derived model is comprehensive enough, in that it affords complete flexibility to the designer to customize the effective properties of the smart composite structure to conform to the requirements of a particular engineering application. This is also evident in the next example considered in this paper.
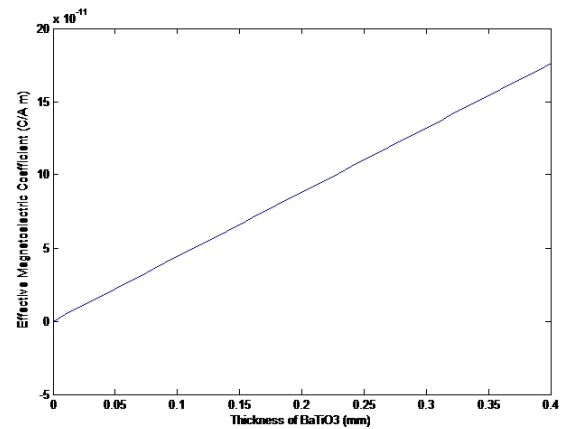

Figure 5: Plot of effective $\langle \xi_{11} \rangle$ magnetoelectric coefficient vs. thickness of the BaTiO$_3$ laminae.

4 Applications of the General Model – Wafer-reinforced Smart Composite Plates

The following examples will be concerned with a different type of structure, namely a wafer-reinforced magneto-electric plate, shown in Fig. 6. For generality we will assume that the material of the base-plate is different than that of the ribs. For example, the base-plate may be elastic or piezomagnetic and the ribs may be piezoelectric. Each constituent material may be assumed to be orthotropic. We are interested in calculating the effective elastic, piezoelectric, thermal expansion, dielectric permittivity, magneto-electric, pyroelectric etc coefficients for this structure.

A solution of the local problems relevant to this kind of geometry may be found assuming that the thickness of each of the three elements of the unit cell is small in comparison with the other two dimensions, i.e.

$$ t_1 \ll h_2, \quad t_2 \ll h_1, \quad H \sim h_1, h_2. \tag{4.1} $$

The local problems can then be approximately solved for each of the unit cell elements assuming that the discontinuities at the joints are highly localized. Consequently, the local problems can be solved independently for regions Ω_1, Ω_2 and Ω_3 as shown in Fig. 7. Fig. 7 also depicts the transformed unit cell, showing the microscopic coordinates y_1, y_2, and z.

The analytical procedure followed in this example is similar to its counterpart in the previous example. First of all, the unit cell problems are simplified in each of the three regions of the unit cell. In particular, periodicity conditions in y_1 and y_2 reduce the pertinent partial differential equations in Region 3 to ordinary differential equations in z. Likewise, since Region 1 is thin and entirely oriented in the y_2 direction it is characterized by independence in y_2. Hence, the corresponding unit cell problem is reduced from a partial differential equation in variables y_1, y_2, and z into one involving y_1 and z only. Similarly, the appropriate differential equation for Region 2 is reduced to one involving variables y_2 and z only. The solution of the unit cell problem in each region involves coefficient functions, e.g. $b_{ij}^{k\alpha}$ which in turn are functions of three unknown local functions, e.g. $N_m^{k\alpha}$, $A_{k\alpha}$, and $\Lambda_{k\alpha}$. Since we need three equations to solve for the three unknown local functions, we need to simultaneously consider all three unit cell problems which involve the given local functions. For example, unit cell problems 2.4a, 2.5a and 2.6a must be solved together. Once the local functions are determined, they are back substituted into the expressions for the coefficient functions, Eqs. 2.7a- 2.7c, from which the effective coefficients can be readily obtained after application of the homogenization procedure, Eq. (I-4.5a). The results from each region are then superimposed.

As mentioned above, in following this procedure, one must naturally accept the error incurred at the regions of intersection between the actuators/reinforcements. However, our approximation will be quite accurate, since these regions of intersection are highly localized and do not contribute significantly to the integral over the entire unit cell domain. Essentially, the error incurred will be negligible, if the dimensions of the actuators/reinforcement are much smaller than the spacing between them. As an indication, we note that Kalamkarov [45] developed an asymptotic homogenization model for thin composite plates reinforced with mutually perpendicular wafers and concluded that if the spacing between the unit cells is at least ten times bigger than the thickness of the reinforcements, the error in the values of the effective elastic coefficients incurred by ignoring the regions of overlap between the reinforcements is less than 1%. A complete mathematical justification for this argument in the form of the so-called princi-

ple of the split homogenized operator has been provided by Bakhvalov and Panasenko [43].

(a) Unit Cell Problems 2.4a, 2.5a and 2.6a and Effective Extensional, Piezoelectric and Piezomagnetic Coefficients

We will first tackle unit cell problem 2.4a. If we assume that the structure is piece-wise homogeneous, then the elastic coefficients in each region of Fig. 7 are uniform. As such, in each of Ω_1, Ω_2, Ω_3 the unit cell problem becomes:

$$
\begin{aligned}
&\frac{1}{h_\beta}\frac{\partial \tau_{i\beta}^{\mu\alpha}}{\partial y_\beta} + \frac{\partial \tau_{i3}^{\mu\alpha}}{\partial z} = 0 \\
&\text{with} \quad \tau_{ij}^{\mu\alpha} N_j^\pm = 0 \quad \text{on } Z^\pm \\
&\text{where} \quad \tau_{ij}^{k\alpha} = L_{ijm} N_m^{k\alpha} + M_{ij} A_{k\alpha} + N_{ij} \Lambda_{k\alpha}
\end{aligned}
\tag{4.2a}
$$

Now, recalling Eqs. (I-4.2c) and (I-4.5d), we can write down the boundary condition in Eq. 4.2a in the form of:

$$
\begin{aligned}
&\frac{1}{h_1}\left\{\tau_{i1}^{\mu\alpha} + C_{i1\mu\alpha}\right\} n_{y1}^\pm + \frac{1}{h_2}\left\{\tau_{i2}^{\mu\alpha} + C_{i2\mu\alpha}\right\} n_{y2}^\pm \\
&+ \left\{\tau_{i3}^{\mu\alpha} + C_{i3\mu\alpha}\right\} n_{y3}^\pm = 0 \quad \text{on } Z^\pm
\end{aligned}
\tag{4.2b}
$$

Dropping the "y" subscript and the "±" superscript for simplicity, Eq. 4.2b becomes:

$$
\begin{aligned}
&t_i^{\mu\alpha} + C_{i\beta\mu\alpha}\frac{n_\beta}{h_\beta} + C_{i3\mu\alpha}n_3 = 0 \quad \text{on } Z^\pm \\
&\text{where} \quad t_i^{\mu\alpha} = \tau_{i\beta}^{\mu\alpha}\frac{n_\beta}{h_\beta} + \tau_{i3}^{\mu\alpha}n_3
\end{aligned}
\tag{4.2c}
$$

The elastic $b_{ij}^{k\alpha}$ functions (from which the effective elastic coefficients may be readily determined) are then given by:

$$
b_{ij}^{\mu\alpha} = \tau_{ij}^{\mu\alpha} + C_{ij\mu\alpha}
\tag{4.2d}
$$

In an entirely analogous manner, unit cell problem 2.5a becomes:

$$
\begin{aligned}
&\frac{1}{h_\beta}\frac{\partial \tau_\beta^{\mu\alpha}}{\partial y_\beta} + \frac{\partial \tau_3^{\mu\alpha}}{\partial z} = 0 \\
&\text{with} \quad t^{\mu\alpha} + Q_{\beta\mu\alpha}\frac{n_\beta}{h_\beta} + Q_{3\mu\alpha}n_3 = 0 \quad \text{on } Z^\pm \\
&\text{where} \quad \tau_j^{k\alpha} = L_{jm}N_m^{k\alpha} - M_j A_{k\alpha} - N_j \Lambda_{k\alpha} \\
&\text{and} \quad t^{\mu\alpha} = \tau_\beta^{\mu\alpha}\frac{n_\beta}{h_\beta} + \tau_3^{\mu\alpha}n_3
\end{aligned}
\tag{4.3a}
$$

This problem will be solved in each of the regions Ω_1, Ω_2, and Ω_3 separately and will yield the in-plane $\eta_j^{k\alpha}$ piezomagnetic functions (which will later give the effective piezomagnetic coefficients) according to:

$$
\eta_j^{\mu\alpha} = \tau_j^{\mu\alpha} + Q_{j\mu\alpha}
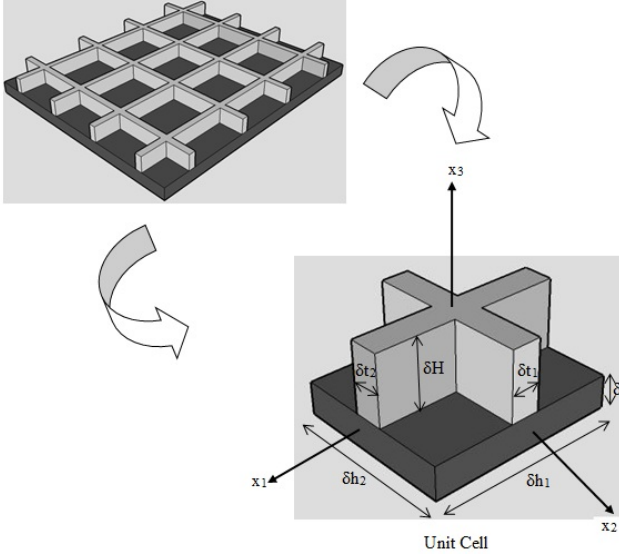\tag{4.3b}
$$

Figure 6: Thin magnetoelectric wafer-reinforced plate and its periodicity cell.

Finally, the third unit cell problem of the group, Eq. 2.6a becomes:

$$\frac{1}{h_\beta}\frac{\partial \pi_\beta^{\mu\alpha}}{\partial y_\beta} + \frac{\partial \pi_3^{\mu\alpha}}{\partial z} = 0$$

$$\text{with} \quad r^{\mu\alpha} + e_{\beta\mu\alpha}\frac{n_\beta}{h_\beta} + e_{3\mu\alpha}n_3 = 0 \quad \text{on } Z^{\pm} \quad (4.4a)$$

$$\text{where} \quad \pi_j^{k\alpha} = L_{jm}^* N_m^{k\alpha} - M_j^* A_{k\alpha} - N_j^* \Lambda_{k\alpha}$$

$$\text{and} \quad r^{\mu\alpha} = \pi_\beta^{\mu\alpha}\frac{n_\beta}{h_\beta} + \pi_3^{\mu\alpha}n_3$$

Again, this problem will be solved in each of the regions Ω_1, Ω_2, and Ω_3 separately and will yield the in-plane $\delta_j^{k\alpha}$ piezoelectric functions (which will later give the effective piezoelectric coefficients) according to:

$$\delta_j^{\mu\alpha} = \pi_j^{\mu\alpha} + e_{j\mu\alpha} \quad (4.4b)$$

    As was the case of the laminate of the previous example, we expect coupled solutions of the current unit cell problems. Hence, Eqs. 4.2a- 4.2c will be solved in each region simultaneously with the corresponding problems in Eqs. 4.3a and 4.4a. We begin by setting up the boundary conditions in each region.

    (i) Region Ω_3.
This is defined by $-1/2 < y_1 < 1/2$, $-1/2 < y_2 < 1/2$, $-1/2 < z < 1/2$, and boundary conditions must be supplied on $z = \pm 1/2$ where $n_1 = n_2 = 0$, $n_3 = 1$. Thus, from Eqs. 4.2a, 4.2c, 4.3a and 4.4a, and keeping in mind that we are dealing with orthotropic materials, see Eq. 3.1, the
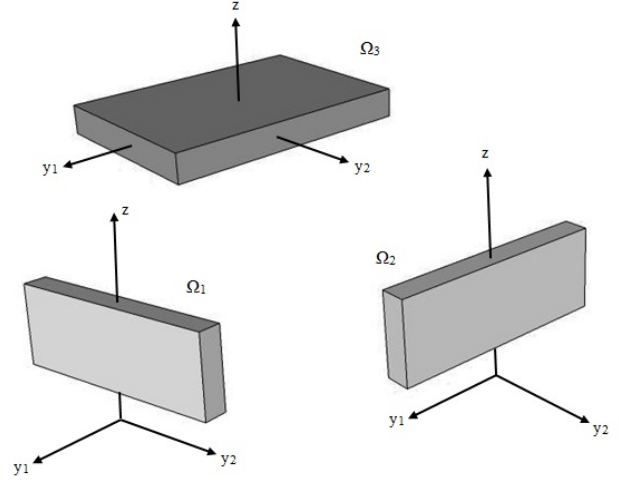

Figure 7: Unit cell of smart wafer and individual elements.

boundary conditions become:

$$\left.\begin{array}{l} t_\alpha^{\lambda\mu} = t_3^{12} = 0 \Rightarrow \\ \tau_{13}^{\lambda\mu} = \tau_{23}^{\lambda\mu} = \tau_{33}^{12} = 0 \\ t_3^{11} = -C_{13}, \quad t_3^{22} = -C_{23} \\ \tau_{33}^{11} = -C_{13} \quad \text{and} \quad \tau_{33}^{22} = -C_{23} \end{array}\right\} \text{on } z = \pm 1/2 \quad (4.5a)$$

$$\begin{array}{l} t^{11} = -Q_{31}, \quad t^{22} = -Q_{32}, \quad t^{12} = 0 \quad \tau_3^{11} = -Q_{31}, \\ \tau_3^{22} = -Q_{32}, \quad \tau_3^{22} = 0 \quad \text{on } z = \pm 1/2 \end{array}$$
$$(4.5b)$$

$$\begin{array}{l} r^{11} = -e_{31}, \quad r^{22} = -e_{32}, \quad r^{12} = 0 \quad \pi_3^{11} = -e_{31}, \\ \pi_3^{22} = -e_{32}, \quad \pi_3^{22} = 0 \quad \text{on } z = \pm 1/2 \end{array}$$
$$(4.5c)$$

(ii) Region Ω_1.
This region is defined by $-\delta_1/2 < y_1 < \delta_1/2$, $-1/2 < y_1 < \delta_1/2 < y_2 < 1/2$, and $1/2 < z < 1/2 + H$. Therefore, boundary conditions must be supplied on $z = 1/2$, $z = 1/2 + H$, where $n_1 = n_2 = 0$, $n_3 = 1$ and on $y_1 = \pm \delta_1/2$ where $n_2 = n_3 = 0$, $n_1 = 1$. Thus, using 4.2a, 4.2c, 4.3a and 4.4a, the boundary conditions become:

$$\left.\begin{array}{l} t_1^{11} = \frac{-C_{11}}{h_1}, \qquad t_1^{22} = \frac{-C_{12}}{h_1}, \\ t_2^{12} = \frac{-C_{66}}{h_1}, \quad t_1^{12} = t_2^{11} = \\ = t_2^{22} = t_3^{\lambda\mu} = 0 \\ \tau_{11}^{11} = -C_{11}, \quad \tau_{11}^{22} = -C_{12}, \\ \tau_{12}^{12} = -C_{66}, \quad \tau_{11}^{12} = \tau_{12}^{11} = \\ = \tau_{12}^{22} = \tau_{13}^{\lambda\mu} = 0 \end{array}\right\} \text{on } y_1 = \pm\delta_1/2$$

$$\left.\begin{array}{l} t_3^{11} = -C_{13}, \quad t_3^{22} = -C_{23}, \\ t_\alpha^{\lambda\mu} = t_3^{12} = 0 \\ \tau_{33}^{11} = -C_{13}, \quad \tau_{33}^{22} = -C_{23}, \\ \tau_{\alpha3}^{\lambda\mu} = \tau_{33}^{12} = 0 \end{array}\right\} \begin{array}{l} \text{on } z = 1/2, \\ 1/2 + H \end{array}$$

$$(4.5d)$$

$$t^{\lambda\mu} = 0 \quad \Rightarrow \quad \tau_1^{\lambda\mu} = 0 \quad \text{on } y_1 = \pm\delta_1/2$$
$$t^{\lambda\lambda} = -Q_{3\lambda}, \quad t^{12} = 0 \quad \tau_3^{11} = -Q_{31},$$
$$\tau_3^{22} = -Q_{32}, \quad \tau_3^{12} = 0 \quad \text{on } z = 1/2, \ 1/2 + H \tag{4.5e}$$

$$r^{\lambda\mu} = 0 \quad \Rightarrow \quad \pi_1^{\lambda\mu} = 0 \quad \text{on } y_1 = \pm\delta_1/2$$
$$r^{\lambda\lambda} = -e_{3\lambda}, \quad r^{12} = 0 \quad \pi_3^{11} = -e_{31},$$
$$\pi_3^{22} = -e_{32}, \quad \pi_3^{12} = 0 \quad \text{on } z = 1/2, \ 1/2 + H \tag{4.5f}$$

(iii) Region Ω_2.

This region is defined by $-\delta_1/2 < y_2 < \delta_1/2, \quad -1/2 < y_1 < 1/2$ and $1/2 < z < 1/2 + H$. Therefore, boundary conditions must be supplied on $z = \frac{1}{2}$, $z = 1/2 + H$, where $n_1 = n_2 = 0$, $n_3 = 1$ and on $y_2 = \pm \delta_2/2$ where $n_1 = n_3 = 0$, $n_2 = 1$. Thus, using 4.2a, 4.2c, 4.3a and 4.4a, the boundary conditions become:

$$\left.\begin{aligned}
&t_2^{11} = \frac{-C_{12}}{h_2}, \qquad t_2^{22} = \frac{-C_{22}}{h_2}, \\
&t_1^{12} = \frac{-C_{66}}{h_2}, \\
&t_2^{12} = t_1^{11} = t_1^{22} = t_3^{\lambda\mu} = 0 \\
&\tau_{22}^{11} = -C_{12}, \quad \tau_{22}^{22} = -C_{22}, \\
&\tau_{12}^{12} = -C_{66}, \\
&\tau_{22}^{12} = \tau_{12}^{11} = \tau_{12}^{22} = \tau_{23}^{\lambda\mu} = 0
\end{aligned}\right\} \begin{aligned}&\text{on } y_1 = \\ &= \pm\delta_1/2\end{aligned}$$

$$\left.\begin{aligned}
&t_3^{11} = -C_{13}, \quad t_3^{22} = -C_{23}, \\
&t_\alpha^{\lambda\mu} = t_3^{12} = 0 \\
&\tau_{33}^{11} = -C_{13}, \quad \tau_{33}^{22} = -C_{23}, \\
&\tau_{\alpha3}^{\lambda\mu} = \tau_{33}^{12} = 0
\end{aligned}\right\} \begin{aligned}&\text{on } z = 1/2, \\ &1/2 + H\end{aligned}$$

$$\tag{4.5g}$$

$$t^{\lambda\mu} = 0 \quad \Rightarrow \quad \tau_2^{\lambda\mu} = 0 \quad \text{on } y_2 = \pm\delta_2/2$$
$$t^{\lambda\lambda} = -Q_{3\lambda}, \quad t^{12} = 0 \quad \tau_3^{11} = -Q_{31}, \quad ,$$
$$\tau_3^{22} = -Q_{32}, \tau_3^{12} = 0 \quad \text{on } z = 1/2, \ 1/2 + H \tag{4.5h}$$

$$r^{\lambda\mu} = 0 \quad \Rightarrow \quad \pi_2^{\lambda\mu} = 0 \quad \text{on } y_2 = \pm\delta_2/2$$
$$r^{\lambda\lambda} = -e_{3\lambda}, \quad r^{12} = 0 \quad \pi_3^{11} = -e_{31}, ,$$
$$\pi_3^{22} = -e_{32}, \pi_3^{12} = 0 \quad \text{on } z = 1/2, \ 1/2 + H \tag{4.5i}$$

We are now ready to solve the unit cell problems in Eqs. 4.2a, 4.3a and 4.4a. We will begin with the τ_{ij}^{22}, τ_i^{22}, and π_i^{22} problems.

Region Ω_3. Because of periodicity in y_1 and y_2, and considering differential equations 4.2a and boundary conditions 4.5a we have:

$$\tau_{13}^{22} = \tau_{23}^{22} = 0, \quad \tau_{33}^{22} = -C_{23} \quad \text{in } \Omega_3 \tag{4.6a}$$

The latter expression in Eq. 4.6a gives, on account of the corresponding definition in Eq. 4.2a and the differential operators (I-5.2a), the following equation:

$$C_{33} \frac{\partial N_3^{22}}{\partial z} + e_{33} \frac{\partial A_{22}}{\partial z} + Q_{33} \frac{\partial \Lambda_{22}}{\partial z} = -C_{23} \quad \text{in } \Omega_3 \tag{4.6b}$$

Similarly, from the unit cell problem 4.3a and boundary conditions 4.5b we arrive at

$$\tau_3^{22} = -Q_{32} \quad \text{in } \Omega_3 \tag{4.6c}$$

which, on account of the pertinent definition in Eq. 4.3a and the differential operators (I-5.2a), gives:

$$Q_{33} \frac{\partial N_3^{22}}{\partial z} - \lambda_{33} \frac{\partial A_{22}}{\partial z} - \mu_{33} \frac{\partial \Lambda_{22}}{\partial z} = -Q_{32} \quad \text{in } \Omega_3 \tag{4.6d}$$

In an analogous manner, unit cell problem 4.4a and boundary conditions 4.5c give,

$$\pi_3^{22} = -e_{32} \quad \text{in } \Omega_3 \tag{4.6e}$$

and

$$e_{33} \frac{\partial N_3^{22}}{\partial z} - \varepsilon_{33} \frac{\partial A_{22}}{\partial z} - \lambda_{33} \frac{\partial \Lambda_{22}}{\partial z} = -e_{32} \quad \text{in } \Omega_3 \tag{4.6f}$$

The solution of the linear system defined by Eqs. 4.6b, 4.6d and 4.6f is:

$$\begin{aligned}
\frac{\partial N_3^{22}}{\partial z} &= -\frac{(Q_{32}\varepsilon_{33} - \lambda_{33}e_{32})Q_{33} - \lambda_{33}^2 C_{23} - \lambda_{33}e_{33}Q_{32}}{\mu_{33}C_{33}\varepsilon_{33} - \lambda_{33}^2 C_{23} + Q_{33}^2\varepsilon_{33} - 2\lambda_{33}e_{33}Q_{33} + e_{33}^2\mu_{33}} + \\
&\quad + \frac{\mu_{33}e_{33}e_{32} + \mu_{33}C_{33}\varepsilon_{33}}{\mu_{33}C_{33}\varepsilon_{33} - \lambda_{33}^2 C_{23} + Q_{33}^2\varepsilon_{33} - 2\lambda_{33}e_{33}Q_{33} + e_{33}^2\mu_{33}} \\
&= \frac{\hat{\Pi}_2}{\hat{\Pi}_1} \\
\frac{\partial A_{22}}{\partial z} &= \frac{(Q_{32}e_{33} + \lambda_{33}C_{32})Q_{33} + Q_{33}^2 e_{32} - \lambda_{33}C_{33}Q_{32}}{\hat{\Pi}_1} + \\
&\quad + \frac{-\mu_{33}e_{33}C_{32} + \mu_{33}C_{33}e_{33}}{\hat{\Pi}_1} = \frac{\hat{\Pi}_3}{\hat{\Pi}_1} \\
\frac{\partial \Lambda_{22}}{\partial z} &= \frac{(C_{32}\varepsilon_{33} + e_{33}e_{32})Q_{33} + e_{33}^2 Q_{32} - \lambda_{33}C_{33}e_{32}}{\hat{\Pi}_1} + \\
&\quad + \frac{Q_{32}\varepsilon_{33}C_{33} + \lambda_{33}C_{23}e_{33}}{\hat{\Pi}_1} = \frac{\hat{\Pi}_4}{\hat{\Pi}_1}
\end{aligned}$$

$$\tag{4.6g}$$

We observe that these expressions are the same as those in Eqs. 3.2f − 3.2h after letting $\mu = \alpha = 2$. Using these solutions, functions $\tau_{ij}^{\lambda\mu}$, $\tau_i^{\lambda\mu}$, $\pi_i^{\lambda\mu}$ are readily determined as follows:

$$\left.\begin{aligned}
&\tau_{11}^{22} = C_{13} \frac{\hat{\Pi}_2}{\hat{\Pi}_1} + e_{31} \frac{\hat{\Pi}_3}{\hat{\Pi}_1} + Q_{31} \frac{\hat{\Pi}_4}{\hat{\Pi}_1}, \\
&\tau_{22}^{22} = C_{23} \frac{\hat{\Pi}_2}{\hat{\Pi}_1} + e_{32} \frac{\hat{\Pi}_3}{\hat{\Pi}_1} + Q_{32} \frac{\hat{\Pi}_4}{\hat{\Pi}_1}, \\
&\tau_{33}^{22} = -C_{23}, \\
&\tau_{\alpha3}^{22} = \tau_{12}^{22} = 0, \quad \tau_3^{22} = -Q_{32}, \\
&\tau_1^{22} = \tau_2^{22} = 0, \quad \pi_3^{22} = -e_{32}, \\
&\pi_1^{22} = \pi_2^{22} = 0
\end{aligned}\right\} \text{in } \Omega_3 \tag{4.7}$$

Region Ω_1. In this region we have independence of the y_2 coordinate, since the element is oriented entirely in the y_2 direction. Thus, from differential equations 4.2a and boundary conditions 4.5d we get:

$$\tau_{13}^{22} = \tau_{23}^{22} = \tau_{12}^{22} = 0, \quad \tau_{11}^{22} = -C_{12},$$
$$\tau_{33}^{22} = -C_{23} \quad \text{in } \Omega_1 \tag{4.8a}$$

The latter two expressions in Eq. 4.8a give, on account of the corresponding definitions in Eq. 4.2a and the differential operators (I-5.2a), the following equations:

$$\left.\begin{array}{l} \dfrac{1}{h_1}C_{11}\dfrac{\partial N_1^{22}}{\partial y_1}+C_{13}\dfrac{\partial N_3^{22}}{\partial z}+ \\[2mm] +e_{31}\dfrac{\partial A_{22}}{\partial z}+Q_{31}\dfrac{\partial \Lambda_{22}}{\partial z}=-C_{12} \\[2mm] \dfrac{1}{h_1}C_{13}\dfrac{\partial N_1^{22}}{\partial y_1}+C_{33}\dfrac{\partial N_3^{22}}{\partial z} \\[2mm] +e_{33}\dfrac{\partial A_{22}}{\partial z}+Q_{33}\dfrac{\partial \Lambda_{22}}{\partial z}=-C_{23} \end{array}\right\} \text{ in } \Omega_1 \qquad (4.8b)$$

Similarly, from the unit cell problem 4.3a and boundary conditions 4.5e we arrive at

$$\tau_3^{22}=-Q_{32}, \quad \tau_1^{22}=0 \quad \text{in } \Omega_1 \qquad (4.8c)$$

which, on account of the pertinent definition in Eq. 4.3a and the differential operators (I-5.2a), gives:

$$\dfrac{1}{h_1}Q_{31}\dfrac{\partial N_1^{22}}{\partial y_1}+Q_{33}\dfrac{\partial N_3^{22}}{\partial z}-\lambda_{33}\dfrac{\partial A_{22}}{\partial z}+$$
$$-\mu_{33}\dfrac{\partial \Lambda_{22}}{\partial z}=-Q_{32} \quad \text{in } \Omega_1 \qquad (4.8d)$$

Realizing that we need one more equation, we turn our attention to unit cell problem 4.4a and boundary conditions 4.5f to get,

$$\pi_3^{22}=-e_{32}, \quad \pi_1^{22}=0 \quad \text{in } \Omega_1 \qquad (4.8e)$$

and

$$\dfrac{1}{h_1}e_{31}\dfrac{\partial N_1^{22}}{\partial y_1}+e_{33}\dfrac{\partial N_3^{22}}{\partial z}-\varepsilon_{33}\dfrac{\partial A_{22}}{\partial z}-\lambda_{33}\dfrac{\partial \Lambda_{22}}{\partial z}=$$
$$=-e_{32} \quad \text{in } \Omega_1$$
$$(4.8f)$$

Eqs. 4.8b, 4.8d and 4.8f represent a system of four linear equations in four unknowns. The solution may be given as:

$$\dfrac{\partial N_1^{22}}{\partial y_1}=h_1\dfrac{\hat{\Pi}_6}{\hat{\Pi}_5}, \quad \dfrac{\partial N_3^{22}}{\partial z}=\dfrac{\hat{\Pi}_7}{\hat{\Pi}_5},$$
$$\dfrac{\partial A_{22}}{\partial z}=\dfrac{\hat{\Pi}_8}{\hat{\Pi}_5}, \quad \dfrac{\partial \Lambda_{22}}{\partial z}=\dfrac{\hat{\Pi}_9}{\hat{\Pi}_5} \quad \text{where} \qquad (4.9a)$$

$$\hat{\Pi}_5=\begin{bmatrix}(-e_{33}^2-\varepsilon_{33}C_{33})Q_{31}^2+(2C_{33}e_{31}\lambda_{33}+ \\ +2\varepsilon_{33}Q_{33}C_{13}-2C_{13}e_{33}\lambda_{33}+ \\ +2e_{31}Q_{33}e_{33})Q_{31}+ \\ -e_{31}^2C_{33}\mu_{33}-Q_{33}^2C_{11}\varepsilon_{33}+\lambda_{33}^2C_{11}C_{33}+ \\ +C_{13}^2\mu_{33}\varepsilon_{33}-Q_{33}^2e_{31}^2-C_{13}^2\lambda_{33}^2+ \\ -2C_{13}Q_{33}e_{31}\lambda_{33}-C_{11}\mu_{33}e_{33}^2+ \\ +2\mu_{33}C_{13}e_{31}e_{33}+ \\ +2C_{11}\lambda_{33}Q_{33}e_{33}-C_{33}C_{11}\varepsilon_{33}\mu_{33}\end{bmatrix}$$
$$(4.9b)$$

$$\hat{\Pi}_6=\begin{bmatrix}(C_{23}e_{33}\lambda_{33}-C_{23}\varepsilon_{33}Q_{33}+C_{33}e_{32}\lambda_{33}+ \\ +Q_{32}\varepsilon_{33}C_{33}+e_{33}^2Q_{32}-e_{33}Q_{33}e_{32})Q_{31}+ \\ +Q_{33}C_{13}\lambda_{33}e_{33}+C_{23}Q_{33}\lambda_{33}e_{31}+ \\ -C_{23}\mu_{33}e_{33}e_{31}-2e_{33}\lambda_{33}Q_{33}C_{12}+ \\ C_{33}\mu_{33}e_{32}e_{31}-\lambda_{33}^2C_{33}C_{12}+C_{33}C_{12}\mu_{33}\varepsilon_{33}+ \\ +e_{33}^2\mu_{33}C_{12}+e_{33}C_{13}\lambda_{33}Q_{32}- \\ e_{33}C_{13}\mu_{33}e_{32}+Q_{33}^2e_{31}e_{32}+Q_{33}^2C_{12}\varepsilon_{33}+ \\ -Q_{33}C_{13}Q_{32}e_{33}+\lambda_{33}^2C_{23}C_{13}- \\ C_{33}e_{31}\lambda_{33}Q_{32}-e_{33}Q_{33}e_{31}Q_{32}\end{bmatrix}$$
$$(4.9c)$$

$$\hat{\Pi}_7=\begin{bmatrix}(e_{33}\lambda_{33}C_{12}-2C_{23}e_{31}\lambda_{33}-e_{31}e_{33}Q_{32}+ \\ +C_{13}e_{32}\lambda_{33}-C_{12}\varepsilon_{33}Q_{33}-e_{31}Q_{33}e_{32}- \\ Q_{32}\varepsilon_{33}C_{13})Q_{31}+(C_{23}\varepsilon_{33}+e_{33}e_{32})Q_{31}^2+ \\ +C_{11}e_{33}\mu_{33}e_{32}+C_{11}Q_{33}Q_{32}\varepsilon_{33}- \\ C_{11}Q_{33}\lambda_{33}e_{32}+C_{11}C_{23}\mu_{33}\varepsilon_{33}+ \\ -C_{11}e_{33}\lambda_{33}Q_{32}-\lambda_{33}^2C_{11}C_{23}+e_{31}^2C_{23}\mu_{33} \\ +C_{13}e_{31}\lambda_{33}Q_{32}-e_{33}\mu_{33}e_{31}C_{12}+ \\ -C_{12}\mu_{33}C_{13}\varepsilon_{33}-C_{13}\mu_{33}e_{31}e_{32}+ \\ +\lambda_{33}^2C_{13}C_{12}+Q_{33}e_{31}\lambda_{33}C_{12}+Q_{32}Q_{33}e_{31}^2\end{bmatrix}$$
$$(4.9d)$$

$$\hat{\Pi}_8=\begin{bmatrix}(-Q_{33}e_{33}C_{12}-C_{13}e_{33}Q_{32}-C_{23}e_{31}Q_{33}+ \\ -C_{33}\lambda_{33}C_{12}+2e_{32}Q_{33}C_{13}+e_{31}Q_{32}C_{33}+ \\ \lambda_{33}C_{23}C_{13})Q_{31}+(C_{23}e_{33}-C_{33}e_{32})Q_{31}^2+ \\ +C_{33}e_{31}\mu_{33}C_{12}+Q_{33}^2e_{31}C_{12}+ \\ C_{33}C_{11}\lambda_{33}Q_{32}-C_{13}^2\lambda_{33}Q_{32}+C_{13}^2\mu_{33}e_{32}+ \\ +C_{11}C_{23}\mu_{33}e_{33}-C_{11}C_{33}\mu_{33}e_{32}+ \\ -C_{11}Q_{33}^2e_{32}+C_{11}Q_{33}e_{33}Q_{32}+ \\ -C_{13}Q_{33}e_{31}Q_{32}+\lambda_{33}Q_{33}C_{13}C_{12}+ \\ -C_{13}\mu_{33}e_{33}C_{12}-C_{11}\lambda_{33}Q_{33}C_{23}+ \\ -\mu_{33}C_{13}e_{31}C_{23}\end{bmatrix}$$
$$(4.9e)$$

$$\hat{\Pi}_9=\begin{bmatrix}(-e_{33}e_{31}C_{23}-C_{13}e_{33}e_{32}+ \\ +C_{33}C_{12}\varepsilon_{33}+C_{12}e_{33}^2 \\ +C_{33}e_{31}e_{32}-C_{23}C_{13}\varepsilon_{33})Q_{31}+ \\ C_{33}C_{11}\lambda_{33}e_{32}-C_{33}C_{11}Q_{32}\varepsilon_{33}+ \\ -e_{31}^2Q_{32}C_{33}-C_{13}Q_{33}C_{12}\varepsilon_{33}+ \\ -C_{33}\lambda_{33}C_{12}e_{31}+2C_{13}Q_{32}e_{31}e_{33}+ \\ +C_{11}Q_{33}e_{32}e_{33}-C_{11}\lambda_{33}e_{33}C_{23}+ \\ +C_{11}Q_{33}C_{23}\varepsilon_{33}-C_{11}e_{33}^2Q_{32}+ \\ -Q_{33}e_{33}e_{31}C_{12}+\lambda_{33}e_{31}C_{13}C_{23}+ \\ -C_{13}^2\lambda_{33}e_{32}-C_{13}Q_{33}e_{31}e_{32}+ \\ +Q_{33}e_{31}^2C_{23}+ \\ Q_{32}C_{13}^2\varepsilon_{33}+\lambda_{33}C_{13}e_{33}C_{12}\end{bmatrix} \quad (4.9f)$$

Using these solutions, functions $\tau_{ij}^{\lambda\mu}$, $\tau_i^{\lambda\mu}$, $\pi_i^{\lambda\mu}$ are readily determined as follows:

$$
\left.
\begin{aligned}
&\tau_{11}^{22}= -C_{12}, \quad \tau_{22}^{22}= C_{12}\frac{\hat{\Pi}_6}{\hat{\Pi}_5}+ \\
&+C_{23}\frac{\hat{\Pi}_7}{\hat{\Pi}_5}+e_{32}\frac{\hat{\Pi}_8}{\hat{\Pi}_5}+Q_{32}\frac{\hat{\Pi}_9}{\hat{\Pi}_5}, \\
&\tau_{33}^{22}= -C_{23}, \quad \tau_{\alpha3}^{22}= \tau_{12}^{22}= 0 \\
&\tau_3^{22}= -Q_{32}, \quad \tau_1^{22}= \tau_2^{22}= 0, \\
&\pi_3^{22}= -e_{32}, \quad \pi_1^{22}= \pi_2^{22}= 0
\end{aligned}
\right\} \text{ in } \Omega_1 \qquad (4.10)
$$

Region Ω_2. In this region we have independence of the y_1 coordinate since the element is oriented entirely in the y_1 direction. Thus, the solution of differential equations 4.2a and boundary conditions 4.5g gives:

$$
\tau_{13}^{22}= \tau_{23}^{22}= \tau_{12}^{22}= 0, \quad \tau_{11}^{22}= -C_{22}, \quad \tau_{33}^{22}= -C_{23} \quad (4.11a)
$$
in Ω_2

The latter two expressions in Eq. 4.11a give, on account of the corresponding definitions in Eq. 4.2a and the differential operators (I-5.2a), the following equations:

$$
\left.
\begin{aligned}
&\frac{1}{h_2}C_{22}\frac{\partial N_2^{22}}{\partial y_2}+C_{23}\frac{\partial N_3^{22}}{\partial z}+ \\
&+e_{32}\frac{\partial A_{22}}{\partial z}+Q_{32}\frac{\partial \Lambda_{22}}{\partial z}= -C_{22} \\
&\frac{1}{h_1}C_{23}\frac{\partial N_1^{22}}{\partial y_2}+C_{33}\frac{\partial N_3^{22}}{\partial z}+ \\
&+e_{33}\frac{\partial A_{22}}{\partial z}+Q_{33}\frac{\partial \Lambda_{22}}{\partial z}= -C_{23}
\end{aligned}
\right\} \text{ in } \Omega_2 \qquad (4.11b)
$$

We need two more equations in order to be able to solve for the unknown functions. Therefore, we resort to unit cell problem 4.3a and boundary conditions 4.5h to arrive at:

$$
\tau_3^{22}= -Q_{32}, \quad \tau_2^{22}= 0 \quad \text{in } \Omega_2 \qquad (4.11c)
$$

On account of the pertinent definition in Eq. 4.3a and the differential operators (I-5.2a), the first expression in Eq. 4.11c gives:

$$
\frac{1}{h_2}Q_{32}\frac{\partial N_2^{22}}{\partial y_2}+Q_{33}\frac{\partial N_3^{22}}{\partial z}-\lambda_{33}\frac{\partial A_{22}}{\partial z}-\mu_{33}\frac{\partial \Lambda_{22}}{\partial z}= \\
= -Q_{32} \quad \text{in } \Omega_2
$$
$$(4.11d)$$

Finally, from unit cell problem 4.4a and boundary conditions 4.5i we get:

$$
\pi_3^{22}= -e_{32}, \quad \pi_2^{22}= 0 \quad \text{in } \Omega_2 \qquad (4.11e)
$$

From the appropriate definition in Eq. 4.4a and the differential operators (I-5.2a) we arrive at:

$$
\frac{1}{h_2}e_{32}\frac{\partial N_2^{22}}{\partial y_2}+e_{33}\frac{\partial N_3^{22}}{\partial z}-\varepsilon_{33}\frac{\partial A_{22}}{\partial z}-\lambda_{33}\frac{\partial \Lambda_{22}}{\partial z}= \\
= -e_{32} \quad \text{in } \Omega_2
$$
$$(4.11f)$$

The solution of system 4.11b, 4.11d, 4.11f is trivial requiring only few algebraic manipulations, and is:

$$
\frac{\partial N_2^{22}}{\partial y_2}= -h_2, \quad \frac{\partial N_3^{22}}{\partial z}=\frac{\partial A_{22}}{\partial z}=\frac{\partial \Lambda_{22}}{\partial z}= 0 \qquad (4.12)
$$

Using these solutions, functions $\tau_{ij}^{\lambda\mu}$, $\tau_i^{\lambda\mu}$, $\pi_i^{\lambda\mu}$ are readily determined as follows:

$$
\left.
\begin{aligned}
&\tau_{11}^{22}= -C_{12}, \\
&\tau_{22}^{22}= -C_{22}, \quad \tau_{33}^{22}= -C_{23}, \quad \tau_{\alpha3}^{22}= \tau_{12}^{22}= 0 \\
&\tau_3^{22}= -Q_{32}, \quad \tau_1^{22}= \tau_2^{22}= 0, \\
&\pi_3^{22}= -e_{32}, \quad \pi_1^{22}= \pi_2^{22}= 0
\end{aligned}
\right\} \text{ in } \Omega_2
$$
$$(4.13)$$

The solution of the τ_{ij}^{11}, τ_i^{11}, and π_i^{11} problems proceeds in much the same way as outlined above. The expressions of the appropriate local functions are given as:

$$
\left.
\begin{aligned}
&\tau_{11}^{11}= C_{13}\frac{\hat{\Pi}_2^*}{\hat{\Pi}_1^*}+e_{31}\frac{\hat{\Pi}_3^*}{\hat{\Pi}_1^*}+Q_{31}\frac{\hat{\Pi}_4^*}{\hat{\Pi}_1^*}, \\
&\tau_{22}^{11}= C_{23}\frac{\hat{\Pi}_2^*}{\hat{\Pi}_1^*}+e_{32}\frac{\hat{\Pi}_3^*}{\hat{\Pi}_1^*}+Q_{32}\frac{\hat{\Pi}_4^*}{\hat{\Pi}_1^*}, \\
&\tau_{33}^{11}= -C_{13} \\
&\tau_{\alpha3}^{11}= \tau_{12}^{11}= 0, \quad \tau_3^{11}= -Q_{31}, \\
&\tau_1^{11}= \tau_2^{11}= 0, \quad \pi_3^{11}= -e_{31}, \quad \pi_1^{11}= \pi_2^{11}= 0
\end{aligned}
\right\} \text{ in } \Omega_3
$$
$$(4.14a)$$

$$
\left.
\begin{aligned}
&\tau_{22}^{11}= -C_{12}, \quad \tau_{11}^{11}= C_{12}\frac{\hat{\Pi}_6^*}{\hat{\Pi}_5^*}+C_{13}\frac{\hat{\Pi}_7^*}{\hat{\Pi}_5^*}+ \\
&+e_{31}\frac{\hat{\Pi}_8^*}{\hat{\Pi}_5^*}+Q_{31}\frac{\hat{\Pi}_9^*}{\hat{\Pi}_5^*}, \quad \tau_{33}^{11}= -C_{13}, \\
&\tau_{\alpha3}^{11}= \tau_{12}^{11}= 0 \\
&\tau_3^{11}= -Q_{31}, \quad \tau_1^{11}= \tau_2^{11}= 0, \\
&\pi_3^{11}= -e_{31}, \quad \pi_1^{11}= \pi_2^{11}= 0
\end{aligned}
\right\} \text{ in } \Omega_2 \quad (4.14b)
$$

$$
\left.
\begin{aligned}
&\tau_{11}^{11}= -C_{11}, \quad \tau_{22}^{11}= -C_{12}, \\
&\tau_{33}^{11}= -C_{13}, \quad \tau_{\alpha3}^{11}= \tau_{12}^{11}= 0 \\
&\tau_3^{11}= -Q_{31}, \quad \tau_1^{11}= \tau_2^{11}= 0, \\
&\pi_3^{11}= -e_{31}, \quad \pi_1^{11}= \pi_2^{11}= 0
\end{aligned}
\right\} \text{ in } \Omega_1 \qquad (4.14c)
$$

Here, material constants $\hat{\Pi}_1^* - \hat{\Pi}_9^*$ are obtained from the corresponding $\hat{\Pi}_1 - \hat{\Pi}_9$ constants given in Eqs. 4.6g, 4.9b- 4.9f, by simply switching index "1" with index "2" and index "2" with index "1" wherever they occur.

The solution of the τ_{ij}^{12}, τ_i^{12}, and π_i^{12} problems proceeds in the same manner. In this case the algebraic systems involved are trivial and the expressions of the appropriate local functions are obtained in a straight-forward fashion as:

$$
\left.
\begin{aligned}
&\tau_{11}^{12}= \tau_{22}^{12}= \tau_{33}^{12}= \tau_{13}^{12}= \\
&= \tau_{23}^{12}= \tau_{12}^{12}= 0, \\
&\tau_1^{12}= \tau_2^{12}= \tau_3^{12}= 0, \\
&\pi_1^{12}= \pi_2^{12}= \pi_3^{12}= 0
\end{aligned}
\right\} \text{ in } \Omega_3 \qquad (4.15a)
$$

$$
\left.
\begin{aligned}
&\tau_{11}^{12}= \tau_{22}^{12}= \tau_{33}^{12}= \tau_{13}^{12}= \tau_{23}^{12}= 0, \\
&\tau_{12}^{12}= -C_{66} \\
&\tau_1^{12}= \tau_2^{12}= \tau_3^{12}= 0, \\
&\pi_1^{12}= \pi_2^{12}= \pi_3^{12}= 0
\end{aligned}
\right\} \text{ in } \Omega_1 \qquad (4.15b)
$$

$$\left.\begin{array}{l} \tau_{11}^{12}=\tau_{22}^{12}=\tau_{33}^{12}=\tau_{13}^{12}=\tau_{23}^{12}=0, \\ \tau_{12}^{12}=-C_{66} \\ \tau_{1}^{12}=\tau_{2}^{12}=\tau_{3}^{12}=0, \\ \pi_{1}^{12}=\pi_{2}^{12}=\pi_{3}^{12}=0 \end{array}\right\} \text{ in } \Omega_2 \quad (4.15c)$$

Before explaining how the effective coefficients may be obtained from the aforementioned local coefficient functions, we will first solve the corresponding unit cell problems associated with the out-of-plane deformation and electric and magnetic field generation of the reinforced magnetoelectric plate.

(b) Unit-Cell Problems 2.4f, 2.5f and 2.6f and Effective Coupling, Out-of-plane Piezoelectric and Out-of-plane Piezomagnetic Coefficients

We now turn our attention to unit cell problems 2.4f, 2.5f and 2.6f. For a piecewise homogeneous unit cell, problem 2.4f may be expressed as:

$$\frac{1}{h_\beta}\frac{\partial \tau_{i\beta}^{(1)\mu\alpha}}{\partial y_\beta} + \frac{\partial \tau_{i3}^{(1)\mu\alpha}}{\partial z} = -C_{33\mu\alpha}\delta_{i3}$$
with $\quad t_i^{(1)\mu\alpha}+zC_{i\beta\mu\alpha}\dfrac{n_\beta}{h_\beta}+zC_{i3\mu\alpha}n_3 = 0 \quad$ on $Z^\pm$
where $\quad \tau_{ij}^{(1)\mu\alpha} = L_{ijm}N_m^{(1)\mu\alpha} + M_{ij}A_{\mu\alpha}^{(1)} + N_{ij}\Lambda_{\mu\alpha}^{(1)}$
and $\quad t_i^{(1)\mu\alpha} = \tau_{i\beta}^{(1)\mu\alpha}\dfrac{n_\beta}{h_\beta}+\tau_{i3}^{(1)\mu\alpha}n_3$

$$(4.16a)$$

The coupling elastic $b_{ij}^{(1)\mu\alpha}$ functions (from which the effective elastic coupling coefficients may be determined) are then given by:

$$b_{ij}^{(1)\mu\alpha}= \tau_{ij}^{(1)\mu\alpha}+zC_{ij\mu\alpha} \quad (4.16b)$$

In an analogous manner, unit cell problem 2.5f becomes:

$$\frac{1}{h_\beta}\frac{\partial \tau_{\beta}^{(1)\mu\alpha}}{\partial y_\beta} + \frac{\partial \tau_{3}^{(1)\mu\alpha}}{\partial z} = -Q_{3\mu\alpha}$$
with $\quad t^{(1)\mu\alpha}+zQ_{\beta\mu\alpha}\dfrac{n_\beta}{h_\beta}+zQ_{3\mu\alpha}n_3 = 0 \quad$ on $Z^\pm$
where $\quad \tau_j^{(1)\mu\alpha} = L_{jm}N_m^{(1)\mu\alpha} - M_jA_{\mu\alpha}^{(1)} - N_j\Lambda_{\mu\alpha}^{(1)}$
and $\quad t^{\mu\alpha} = \tau_{\beta}^{\mu\alpha}\dfrac{n_\beta}{h_\beta}+\tau_{3}^{\mu\alpha}n_3$

$$(4.17a)$$

This problem will be solved in each of the regions Ω_1, Ω_2, and Ω_3 separately and will yield the out-of-plane $a_j^{(1)\mu\alpha}$ piezomagnetic functions (which in turn give the effective out-of-plane piezomagnetic coefficients) according to:

$$a_j^{(1)\mu\alpha}= \tau_j^{(1)\mu\alpha}+zQ_{j\mu\alpha} \quad (4.17b)$$

Finally, the third unit cell problem that will be solved in conjunction with the aforementioned two problems,

Eq. 2.6f, becomes:

$$\frac{1}{h_\beta}\frac{\partial \pi_{\beta}^{(1)\mu\alpha}}{\partial y_\beta} + \frac{\partial \pi_{3}^{(1)\mu\alpha}}{\partial z} = -e_{3\mu\alpha}$$
with $\quad r^{(1)\mu\alpha}+ze_{\beta\mu\alpha}\dfrac{n_\beta}{h_\beta}+ze_{3\mu\alpha}n_3 = 0 \quad$ on $Z^\pm$
where $\quad \pi_j^{(1)\mu\alpha} = L_{jm}^\star N_m^{(1)\mu\alpha} - M_j^\star A_{\mu\alpha}^{(1)} - N_j^\star \Lambda_{\mu\alpha}^{(1)}$
and $\quad r^{(1)\mu\alpha} = \pi_{\beta}^{(1)\mu\alpha}\dfrac{n_\beta}{h_\beta}+\pi_{3}^{(1)\mu\alpha}n_3$

$$(4.18a)$$

Again, this problem will be solved in each of the regions Ω_1, Ω_2, and Ω_3 separately and will yield the out-of-plane $\delta_j^{(1)\mu\alpha}$ piezoelectric functions (which in turn give the effective out-of-plane piezoelectric coefficients) according to:

$$\delta_j^{(1)\mu\alpha}= \pi_j^{(1)\mu\alpha}+ze_{j\mu\alpha} \quad (4.18b)$$

Let us begin by setting up the boundary conditions:

(i) Region Ω_3. As before, boundary conditions must be supplied on $z = \pm 1/2$ where $n_1 = n_2 = 0$, $n_3 = 1$. Thus, from Eqs. 4.16a, 4.17a, and 4.18a, and remembering that we are dealing with orthotropic materials, the boundary conditions become:

$$\begin{array}{ll} \tau_{13}^{(1)\lambda\mu} = \tau_{23}^{(1)\lambda\mu} = \tau_{33}^{(1)12} = 0, & \tau_{33}^{(1)11} = -zC_{13}, \\ \tau_{33}^{(1)22} = -zC_{23} & \text{on } z = \pm 1/2 \end{array} \quad (4.19a)$$

$$\begin{array}{ll} \tau_{3}^{(1)11} = -zQ_{31}, & \tau_{3}^{(1)22} = -zQ_{32}, \\ \tau_{3}^{(1)12} = 0 & \text{on } z = \pm 1/2 \end{array} \quad (4.19b)$$

$$\begin{array}{ll} \pi_{3}^{(1)11} = -zQ_{31}, & \pi_{3}^{(1)22} = -zQ_{32}, \\ \pi_{3}^{(1)12} = 0 & \text{on } z = \pm 1/2 \end{array} \quad (4.19c)$$

(ii) Region Ω_1. Boundary conditions must be supplied on $z = 1/2$, $z = 1/2 +H$, where $n_1 = n_2 = 0$, $n_3 = 1$ and on $y_1 = \pm\delta_1/2$ where $n_2 = n_3 = 0$, $n_1 = 1$. Thus, using Eqs. 4.16a, 4.17a, and 4.18a, the boundary conditions become:

$$\begin{array}{ll} \tau_{11}^{(1)11} = -zC_{11}, & \tau_{11}^{(1)22} = -zC_{12}, \\ \tau_{12}^{(1)12} = -zC_{16}, & \tau_{11}^{(1)12} = \tau_{12}^{(1)11} = \tau_{12}^{(1)22} = \tau_{13}^{(1)\lambda\mu} = 0 \\ \multicolumn{2}{l}{\text{on } y_1 = \pm\delta_1/2} \\ \tau_{33}^{(1)11} = -zC_{13}, & \tau_{33}^{(1)22} = -zC_{23}, \\ \tau_{\alpha 3}^{(1)\lambda\mu} = \tau_{33}^{(1)12} = 0 & \text{on } z = 1/2, \ 1/2+H \end{array}$$

$$(4.20a)$$

$$\begin{array}{ll} \tau_{1}^{(1)\lambda\mu} = 0 & \text{on } y_1 = \pm\delta_1/2 \\ \tau_{3}^{(1)11} = -Q_{31}, & \tau_{3}^{(1)22} = -Q_{32}, \\ \tau_{3}^{(1)12} = 0 & \text{on } z = 1/2, \ 1/2 + H \end{array} \quad (4.20b)$$

$$\begin{array}{ll} \pi_{1}^{(1)\lambda\mu} = 0 & \text{on } y_1 = \pm\delta_1/2 \\ \pi_{3}^{(1)11} = -ze_{31}, & \pi_{3}^{(1)22} = -ze_{32}, \\ \pi_{3}^{(1)12} = 0 & \text{on } z = 1/2+H \end{array} \quad (4.20c)$$

(iii) Region Ω_2. Here, boundary conditions must be supplied on $z = 1/2$, $z = 1/2 +H$, where $n_1 = n_2 = 0$, $n_3 = 1$

and on $y_2 = \pm\delta_2/2$ where $n_1 = n_3 = 0$, $n_2 = 1$. Thus, using Eqs. 4.16a, 4.17a, and 4.18a the boundary conditions become:

$$
\begin{aligned}
&\tau_{22}^{(1)11} = -zC_{12}, \quad \tau_{22}^{(1)22} = -zC_{22}, \\
&\tau_{12}^{(1)12} = -zC_{66}, \quad \tau_{22}^{(1)12} = \tau_{12}^{(1)11} = \tau_{12}^{(1)22} = \tau_{23}^{(1)\lambda\mu} = 0 \\
&on\ y_2 = \pm\delta_2/2 \\
&\tau_{33}^{(1)11} = -zC_{13}, \quad \tau_{33}^{(1)22} = -zC_{23}, \\
&\tau_{\alpha3}^{(1)\lambda\mu} = \tau_{33}^{(1)12} = 0 \quad on\ z = 1/2 + H
\end{aligned}
$$

$$(4.21a)$$

$$
\begin{aligned}
&\tau_2^{(1)\lambda\mu} = 0 \qquad on\ y_2 = \pm\delta_2/2 \\
&\tau_3^{(1)11} = -zQ_{31}, \quad \tau_3^{(1)22} = -zQ_{32}, \\
&\tau_3^{(1)12} = 0 \qquad on\ z = 1/2 + H
\end{aligned}
$$

$$(4.21b)$$

$$
\begin{aligned}
&\pi_2^{(1)\lambda\mu} = 0 \qquad on\ y_2 = \pm\delta_2/2 \\
&\pi_3^{(1)11} = -ze_{31}, \quad \pi_3^{(1)22} = -ze_{32}, \\
&\pi_3^{(1)12} = 0 \qquad on\ z = 1/2 + H
\end{aligned}
$$

$$(4.21c)$$

We are now ready to solve the unit cell problems in Eqs. 4.17a, 4.18a and 4.19a. We will begin with the $\tau_{ij}^{(1)22}$, $\tau_i^{(1)22}$, and $\pi_i^{(1)22}$ functions. Following the same methodology as per the corresponding τ_{ij}^{22}, τ_i^{22}, and π_i^{22} functions we arrive at the following system of equations in region Ω_3.

$$
\begin{bmatrix}
C_{33}\dfrac{\partial N_3^{(1)22}}{\partial z} + e_{33}\dfrac{\partial A_{22}^{(1)}}{\partial z} + Q_{33}\dfrac{\partial \Lambda_{22}^{(1)}}{\partial z} \\[2mm]
Q_{33}\dfrac{\partial N_3^{(1)22}}{\partial z} - \lambda_{33}\dfrac{\partial A_{22}^{(1)}}{\partial z} - \mu_{33}\dfrac{\partial \Lambda_{22}^{(1)}}{\partial z} \\[2mm]
e_{33}\dfrac{\partial N_3^{(1)22}}{\partial z} - \varepsilon_{33}\dfrac{\partial A_{22}^{(1)}}{\partial z} - \lambda_{33}\dfrac{\partial \Lambda_{22}^{(1)}}{\partial z}
\end{bmatrix} =
$$

$$
= -z\begin{bmatrix} C_{23} \\ Q_{32} \\ Q_{32} \end{bmatrix} \quad in\ \Omega_3
$$

$$(4.22a)$$

Comparing this system with Eqs. 4.6b, 4.6d and 4.6f, we observe that the only difference is the presence of the "z" coordinate on the right-hand side. Clearly, this is to be expected, because the three unit cell problems under discussion pertain to out-of-plane deformation of the magneto-electric composite. The solution of Eq. 4.22a is thus readily obtained from its counterpart in Eq. 4.6g by simply multiplying by z. In turn, the local functions τ_{ij}^{22}, τ_i^{22}, π_i^{22} are determined as follows:

$$
\left\{
\begin{aligned}
&\tau_{11}^{(1)22} = z\left(C_{13}\dfrac{\hat{\Pi}_2}{\hat{\Pi}_1} + e_{31}\dfrac{\hat{\Pi}_3}{\hat{\Pi}_1} + Q_{31}\dfrac{\hat{\Pi}_4}{\hat{\Pi}_1}\right), \\[2mm]
&\tau_{22}^{(1)22} = z\left(C_{23}\dfrac{\hat{\Pi}_2}{\hat{\Pi}_1} + e_{32}\dfrac{\hat{\Pi}_3}{\hat{\Pi}_1} + Q_{32}\dfrac{\hat{\Pi}_4}{\hat{\Pi}_1}\right) \\[2mm]
&\tau_{33}^{(1)22} = -zC_{23}, \quad \tau_{\alpha3}^{(1)22} = \tau_{12}^{(1)22} = 0 \\[1mm]
&\tau_3^{(1)22} = -zQ_{32}, \quad \tau_1^{(1)22} = \tau_2^{(1)22} = 0 \\[1mm]
&\pi_3^{(1)22} = -ze_{32}, \quad \pi_1^{(1)22} = \pi_2^{(1)22} = 0
\end{aligned}
\right\} in\ \Omega_3
$$

$$(4.23a)$$

The same conclusion, namely that $\tau_{ij}^{(1)\lambda\mu} = z\tau_{ij}^{(1)\lambda\mu}$, $\tau_i^{(1)\lambda\mu} = z\tau_i^{\lambda\mu}$, $\pi_i^{(1)\lambda\mu} = z\pi_i^{\lambda\mu}$ is also true in regions Ω_1 and Ω_2. Thus:

$$
\left.
\begin{aligned}
&\tau_{11}^{(1)22} = -zC_{12}, \quad \tau_{22}^{(1)22} = \\[1mm]
&= z\left(C_{12}\dfrac{\hat{\Pi}_6}{\hat{\Pi}_5} + C_{23}\dfrac{\hat{\Pi}_7}{\hat{\Pi}_5} + e_{32}\dfrac{\hat{\Pi}_8}{\hat{\Pi}_5} + Q_{32}\dfrac{\hat{\Pi}_9}{\hat{\Pi}_5}\right) \\[2mm]
&\tau_{33}^{(1)22} = -zC_{23}, \quad \tau_{\alpha3}^{(1)22} = \tau_{12}^{(1)22} = 0 \\[1mm]
&\tau_3^{(1)22} = -zQ_{32}, \quad \tau_1^{(1)22} = \tau_2^{(1)22} = 0 \\[1mm]
&\pi_3^{(1)22} = -e_{32}, \quad \pi_1^{(1)22} = \pi_2^{(1)22} = 0
\end{aligned}
\right\} in\ \Omega_1
$$

$$(4.23b)$$

$$
\left.
\begin{aligned}
&\tau_{11}^{(1)22} = -zC_{12}, \quad \tau_{22}^{(1)22} = -zC_{22}, \\[1mm]
&\tau_{33}^{(1)22} = -zC_{23}, \quad \tau_{\alpha3}^{(1)22} = \tau_{12}^{(1)22} = 0 \\[1mm]
&\tau_3^{(1)22} = -zQ_{32}, \quad \tau_1^{(1)22} = \tau_2^{(1)22} = 0, \\[1mm]
&\pi_3^{(1)22} = -e_{32}, \quad \pi_1^{(1)22} = \pi_2^{(1)22} = 0
\end{aligned}
\right\} in\ \Omega_2 \quad (4.23c)
$$

Here, functions $\hat{\Pi}_1$-$\hat{\Pi}_9$ are given in Eqs. 4.6g and 4.9b – 4.9f. Likewise, functions τ_{ij}^{11}, τ_i^{11}, π_i^{11} are obtained in a similar way:

$$
\left.
\begin{aligned}
&\tau_{11}^{(1)11} = z\left(C_{13}\dfrac{\hat{\Pi}_2^\star}{\hat{\Pi}_1^\star} + e_{31}\dfrac{\hat{\Pi}_3^\star}{\hat{\Pi}_1^\star} + Q_{31}\dfrac{\hat{\Pi}_4^\star}{\hat{\Pi}_1^\star}\right), \\[2mm]
&\tau_{22}^{(1)11} = z\left(C_{23}\dfrac{\hat{\Pi}_2^\star}{\hat{\Pi}_1^\star} + e_{32}\dfrac{\hat{\Pi}_3^\star}{\hat{\Pi}_1^\star} + Q_{32}\dfrac{\hat{\Pi}_4^\star}{\hat{\Pi}_1^\star}\right) \\[2mm]
&\tau_{33}^{(1)11} = -zC_{13}, \quad \tau_{\alpha3}^{(1)11} = \tau_{12}^{(1)11} = 0 \\[1mm]
&\tau_3^{(1)11} = -zQ_{31}, \quad \tau_1^{(1)11} = \tau_2^{(1)11} = 0, \\[1mm]
&\pi_3^{(1)11} = -ze_{31}, \quad \pi_1^{(1)11} = \pi_2^{(1)11} = 0
\end{aligned}
\right\} in\ \Omega_3
$$

$$(4.24a)$$

$$
\left.
\begin{aligned}
&\tau_{22}^{(1)11} = -zC_{12}, \quad \tau_{11}^{(1)11} = \\[1mm]
&= z\left(C_{12}\dfrac{\hat{\Pi}_6^\star}{\hat{\Pi}_5^\star} + C_{13}\dfrac{\hat{\Pi}_7^\star}{\hat{\Pi}_5^\star} + e_{31}\dfrac{\hat{\Pi}_8^\star}{\hat{\Pi}_5^\star} + Q_{31}\dfrac{\hat{\Pi}_9^\star}{\hat{\Pi}_5^\star}\right) \\[2mm]
&\tau_{33}^{(1)11} = -zC_{13}, \quad \tau_{\alpha3}^{(1)11} = \tau_{12}^{(1)11} = 0 \\[1mm]
&\tau_3^{(1)11} = -zQ_{31}, \quad \tau_1^{(1)11} = \tau_2^{(1)11} = 0 \\[1mm]
&\pi_3^{(1)11} = -e_{31}, \quad \pi_1^{(1)11} = \pi_2^{(1)11} = 0
\end{aligned}
\right\} in\ \Omega_2 \quad (4.24b)
$$

$$
\left.
\begin{aligned}
&\tau_{11}^{(1)11} = -zC_{11}, \quad \tau_{22}^{(1)11} = -zC_{12}, \\[1mm]
&\tau_{33}^{(1)11} = -zC_{13}, \quad \tau_{\alpha3}^{(1)11} = \tau_{12}^{(1)11} = 0 \\[1mm]
&\tau_3^{(1)11} = -zQ_{31}, \quad \tau_1^{(1)11} = \tau_2^{(1)11} = 0, \\[1mm]
&\pi_3^{(1)11} = -ze_{31}, \quad \pi_1^{(1)11} = \pi_2^{(1)11} = 0
\end{aligned}
\right\} in\ \Omega_1 \quad (4.24c)
$$

In dealing with the $\tau_{ij}^{(1)12}$, $\tau_i^{(1)12}$, $\pi_i^{(1)12}$ functions a slight complication arises. In particular from unit cell problem 4.17a and boundary condition 4.20a we readily arrive at (region Ω_1):

$$
\frac{1}{h_1}\frac{\partial \tau_{12}^{(1)12}}{\partial y_1} + \frac{\partial \tau_{23}^{(1)12}}{\partial z} = 0 \qquad (4.25a)
$$

Expressing $\tau_{12}^{(1)12}$ and $\tau_{23}^{(1)12}$ in terms of the $N_2^{(1)12}$ functions by using the second expression in Eq. 4.16a, we arrive at

Laplace's equation, namely:

$$\frac{1}{h_1^2} C_{66} \frac{\partial^2 N_2^{(1)12}}{\partial y_1^2} + C_{44} \frac{\partial^2 N_2^{(1)12}}{\partial z^2} = 0 \qquad (4.25b)$$

The solution of Eq. 4.25b is obtained in a straightforward manner as:

$$N_2^{(1)12} = -\frac{h_1}{2}[H+1]y_1 +$$

$$+ \frac{2H^3}{\pi^3}\sqrt{\frac{C_{66}}{C_{44}}} \sum_{n=1}^{\infty} \frac{\left[1-(-1)^n\right]\sinh\left(\frac{n\pi h_1}{H}\sqrt{\frac{C_{66}}{C_{44}}}y_1\right)}{n^3 \cosh\left(\frac{C_{66}}{C_{44}}\frac{n\pi\delta_1 h_1}{2H}\right)}$$

$$\cos\left[\frac{n\pi}{H}\left(z-\frac{1}{2}\right)\right] \qquad (4.25c)$$

A similar solution (with the indices "1" and "2" interchanged) is obtained in region Ω_2. Thus, the following solutions are obtained in the three regions of the unit cell:

$$\left.\begin{array}{l}\tau_{ij}^{(1)12} = 0 \\ \tau_i^{(1)12} = 0, \quad \pi_i^{(1)12} = 0\end{array}\right\} \text{ in } \Omega_3 \qquad (4.26a)$$

$$\left.\begin{array}{l}\tau_{11}^{(1)12} = \tau_{22}^{(1)12} = \tau_{33}^{(1)12} = \tau_{13}^{(1)12} = 0, \\[4pt] \tau_1^{(1)12} = \tau_3^{(1)12} = 0, \quad \pi_1^{(1)12} = \pi_3^{(1)12} = 0 \\[4pt] \tau_{12}^{(1)12} = -\frac{C_{66}}{2}[H+1] + \frac{2H}{\pi^2}C_{66}\hat{\Pi}_{10}, \\[4pt] \tau_{23}^{(1)12} = -\sqrt{C_{66}C_{44}}\frac{2H}{\pi^2}\hat{\Pi}_{10}^{\star} \\[4pt] \tau_2^{(1)12} = -Q_{24}\frac{2H}{\pi^2}\sqrt{\frac{C_{66}}{C_{44}}}\hat{\Pi}_{10}^{\star} \\[4pt] \pi_2^{(1)12} = -e_{24}\frac{2H}{\pi^2}\sqrt{\frac{C_{66}}{C_{44}}}\hat{\Pi}_{10}^{\star}\end{array}\right\} \text{ in } \Omega_1$$

$$(4.26b)$$

$$\left.\begin{array}{l}\tau_{11}^{(1)12} = \tau_{22}^{(1)12} = \tau_{33}^{(1)12} = \tau_{23}^{(1)12} = 0, \\[4pt] \tau_2^{(1)12} = \tau_3^{(1)12} = 0, \quad \pi_2^{(1)12} = \pi_3^{(1)12} = 0 \\[4pt] \tau_{12}^{(1)12} = -\frac{C_{66}}{2}[H+1] + \frac{2H}{\pi^2}C_{66}\hat{\Pi}_{11}, \\[4pt] \tau_{13}^{(1)12} = -\sqrt{C_{66}C_{55}}\frac{2H}{\pi^2}\hat{\Pi}_{11}^{\star} \\[4pt] \tau_1^{(1)12} = -Q_{15}\frac{2H}{\pi^2}\sqrt{\frac{C_{66}}{C_{55}}}\hat{\Pi}_{11}^{\star} \\[4pt] \pi_1^{(1)12} = \pi_3^{(1)12} = 0, \\[4pt] \pi_1^{(1)12} = -e_{15}\frac{2H}{\pi^2}\sqrt{\frac{C_{66}}{C_{44}}}\hat{\Pi}_{11}^{\star}\end{array}\right\} \text{ in } \Omega_2$$

$$(4.26c)$$

Here:

$$\hat{\Pi}_{10} = \sum_{n=1}^{\infty} \frac{\left[1-(-1)^n\right]\cosh\left(\frac{n\pi h_1}{H}\sqrt{\frac{C_{44}}{C_{66}}}y_1\right)}{n^2 \cosh\left(\sqrt{\frac{C_{44}}{C_{66}}}\frac{n\pi\delta_1 h_1}{2H}\right)}$$

$$\cos\left[\frac{n\pi}{H}\left(z-\frac{1}{2}\right)\right]$$

$$\hat{\Pi}_{10}^{\star} = \sum_{n=1}^{\infty} \frac{\left[1-(-1)^n\right]\cosh\left(\frac{n\pi h_1}{H}\sqrt{\frac{C_{44}}{C_{66}}}y_1\right)}{n^2 \cosh\left(\sqrt{\frac{C_{44}}{C_{66}}}\frac{n\pi\delta_1 h_1}{2H}\right)}$$

$$\sin\left[\frac{n\pi}{H}\left(z-\frac{1}{2}\right)\right]$$

and $\hat{\Pi}_{11}$ is obtained from $\hat{\Pi}_{10}$, with C_{55} replacing C_{44}, h_2 replacing h_1, δ_2 replacing δ_1, y_2 replacing y_1, $\sinh(\dots)$ replacing $\cosh(\dots)$ and $\sin(\dots)$ replacing $\cos(\dots)$. Likewise, $\hat{\Pi}_{11}^{\star}$ is obtained from $\hat{\Pi}_{10}^{\star}$ by making the same substitutions. It would not be remiss to mention here that, because the materials of choice in this example are orthotropic with the poling/magnetization direction chosen as the z-axis, the $\tau_{ij}^{(1)12}$ problem decouples from its $\tau_i^{(1)12}$, $\pi_i^{(1)12}$ counterparts. Hence, the elastic coefficients in Eqs. 4.26c and 4.26d depend only on elastic parameters, but the piezoelectric and piezomagnetic coefficients in the latter two expressions in Eqs. 4.26c and 4.26d depend on both elastic as well as piezoelectric/piezomagnetic material parameters.

We are now ready to calculate the effective elastic, piezoelectric and piezomagnetic coefficients. We first recall the averaging procedure defined in Eq. (I-4.5a). We can thus easily show the following formulae:

$$\langle 1 \rangle_{\Omega_\alpha} = \int_{\Omega_\alpha} 1 \, dy_1 dy_2 dz = \frac{H t_\alpha}{h_\alpha} = F_\alpha^{(w)},$$

$$\langle 1 \rangle_{\Omega_3} = 1,$$

$$\langle z \rangle_{\Omega_\alpha} = \int_{\Omega_\alpha} z \, dy_1 dy_2 dz = \frac{(H^2+H) t_\alpha}{2h_\alpha} = S_\alpha^{(w)},$$

$$\langle z \rangle_{\Omega_3} = 0,$$

$$\langle z^2 \rangle_{\Omega_\alpha} = \int_{\Omega_\alpha} z^2 \, dy_1 dy_2 dz = \frac{(4H^3+6H^2+3H) t_\alpha}{12h_\alpha} = J_\alpha^{(w)},$$

$$\langle z^2 \rangle_{\Omega_3} = 1/12,$$

$$(4.26d)$$

where $F_1^{(w)}, F_2^{(w)}$ are cross-sectional areas (perpendicular to the orientation of the reinforcement), $S_1^{(w)}, S_2^{(w)}$ are the first moments of the cross-sections, and $J_1^{(w)}, J_2^{(w)}$ are the moments of inertia of the cross-sections of the reinforcing elements Ω_1 and Ω_2 relative to the middle surface of the plate Ω_3. Using these results, as well as Eqs. 4.7, 4.10, 4.13, 4.14a- 4.14c, 4.15a- 4.15c, 4.23a-4.23c, 4.24a- 4.24c, 4.26a- 4.26d and (I-6.3), **the effective extensional elastic coefficients** of the magnetoelectric

wafer are obtained as follows:

$$
\left\langle b_{11}^{11} \right\rangle = \left\{ C_{13}\frac{\hat{\Pi}_2^*}{\hat{\Pi}_1^*} + e_{31}\frac{\hat{\Pi}_3^*}{\hat{\Pi}_1^*} + Q_{31}\frac{\hat{\Pi}_4^*}{\hat{\Pi}_1^*} + C_{11} \right\}^{(\bar{3})} +
$$
$$
+ \left\{ C_{12}\frac{\hat{\Pi}_6^*}{\hat{\Pi}_5^*} + C_{13}\frac{\hat{\Pi}_7^*}{\hat{\Pi}_5^*} + e_{31}\frac{\hat{\Pi}_8^*}{\hat{\Pi}_5^*} + Q_{31}\frac{\hat{\Pi}_9^*}{\hat{\Pi}_5^*} + C_{11} \right\}^{(\bar{2})} F_2^{(w)}
$$
$$
\left\langle b_{22}^{11} \right\rangle = \left\{ C_{23}\frac{\hat{\Pi}_2^*}{\hat{\Pi}_1^*} + e_{32}\frac{\hat{\Pi}_3^*}{\hat{\Pi}_1^*} + Q_{32}\frac{\hat{\Pi}_4^*}{\hat{\Pi}_1^*} + C_{12} \right\}^{(\bar{3})},
$$
$$
\left\langle b_{11}^{22} \right\rangle = \left\{ C_{13}\frac{\hat{\Pi}_2}{\hat{\Pi}_1} + e_{31}\frac{\hat{\Pi}_3}{\hat{\Pi}_1} + Q_{31}\frac{\hat{\Pi}_4}{\hat{\Pi}_1} + C_{12} \right\}^{(\bar{3})}
$$
$$
\left\langle b_{22}^{22} \right\rangle = \left\{ C_{23}\frac{\hat{\Pi}_2}{\hat{\Pi}_1} + e_{32}\frac{\hat{\Pi}_3}{\hat{\Pi}_1} + Q_{32}\frac{\hat{\Pi}_4}{\hat{\Pi}_1} + C_{22} \right\}^{(\bar{3})} +
$$
$$
+ \left\{ C_{12}\frac{\hat{\Pi}_6}{\hat{\Pi}_5} + C_{23}\frac{\hat{\Pi}_7}{\hat{\Pi}_5} + e_{32}\frac{\hat{\Pi}_8}{\hat{\Pi}_5} + Q_{32}\frac{\hat{\Pi}_9}{\hat{\Pi}_5} + C_{22} \right\}^{(\bar{1})} F_1^{(w)}
$$
$$
\left\langle b_{12}^{11} \right\rangle = \left\langle b_{11}^{12} \right\rangle = \left\langle b_{12}^{22} \right\rangle = \left\langle b_{22}^{12} \right\rangle = \left\langle b_{3j}^{\lambda\mu} \right\rangle = 0,
$$
$$
\left\langle b_{12}^{12} \right\rangle = \{C_{66}\}^{(\bar{3})}
$$

$$(4.27a)$$

Here, superscripts $(\bar{1})$, $(\bar{2})$, $(\bar{3})$ following a set of braces, e.g. $\{\ldots\}^{(\bar{1})}$ denote the corresponding region of the unit cell, and the material parameters in the preceding braces pertain to the constituent material of that region. For example, referring to the first expression in Eq. 4.27a, all parameters within the first set of braces refer to the material of the base plate (region Ω_3), and all parameters within the second set of braces refer to region Ω_2. Likewise, the **effective coupling elastic coefficients** are given by:

$$
\left\langle zb_{11}^{11} \right\rangle = \left\langle b_{11}^{(1)11} \right\rangle =
$$
$$
= \left\{ C_{12}\frac{\hat{\Pi}_6^*}{\hat{\Pi}_5^*} + C_{13}\frac{\hat{\Pi}_7^*}{\hat{\Pi}_5^*} + e_{31}\frac{\hat{\Pi}_8^*}{\hat{\Pi}_5^*} + Q_{31}\frac{\hat{\Pi}_9^*}{\hat{\Pi}_5^*} + C_{11} \right\}^{(\bar{2})} S_2^{(w)}
$$
$$
\left\langle zb_{22}^{22} \right\rangle = \left\langle b_{22}^{(1)22} \right\rangle =
$$
$$
= \left\{ C_{12}\frac{\hat{\Pi}_6}{\hat{\Pi}_5} + C_{23}\frac{\hat{\Pi}_7}{\hat{\Pi}_5} + e_{32}\frac{\hat{\Pi}_8}{\hat{\Pi}_5} + Q_{32}\frac{\hat{\Pi}_9}{\hat{\Pi}_5} + C_{22} \right\}^{(\bar{1})} S_1^{(w)}
$$
$$
\left\langle b_{22}^{(1)11} \right\rangle = \left\langle b_{22}^{(1)11} \right\rangle = \left\langle b_{12}^{(1)11} \right\rangle = \left\langle b_{11}^{(1)12} \right\rangle =
$$
$$
= \left\langle b_{12}^{(1)22} \right\rangle = \left\langle b_{22}^{(1)12} \right\rangle = \left\langle b_{3j}^{(1)\lambda\mu} \right\rangle = 0
$$

$$(4.27b)$$

Finally, the effective **bending elastic coefficients** are given as:

$$
\left\langle zb_{11}^{(1)11} \right\rangle = \frac{1}{12} \left\{ C_{13}\frac{\hat{\Pi}_2^*}{\hat{\Pi}_1^*} + e_{31}\frac{\hat{\Pi}_3^*}{\hat{\Pi}_1^*} + Q_{31}\frac{\hat{\Pi}_4^*}{\hat{\Pi}_1^*} + C_{11} \right\}^{(\bar{3})} +
$$
$$
+ \left\{ C_{12}\frac{\hat{\Pi}_6^*}{\hat{\Pi}_5^*} + C_{13}\frac{\hat{\Pi}_7^*}{\hat{\Pi}_5^*} + e_{31}\frac{\hat{\Pi}_8^*}{\hat{\Pi}_5^*} + Q_{31}\frac{\hat{\Pi}_9^*}{\hat{\Pi}_5^*} + C_{11} \right\}^{(\bar{2})} J_2^{(w)}
$$
$$
\left\langle zb_{22}^{(1)11} \right\rangle = \frac{1}{12} \left\{ C_{23}\frac{\hat{\Pi}_2^*}{\hat{\Pi}_1^*} + e_{32}\frac{\hat{\Pi}_3^*}{\hat{\Pi}_1^*} + Q_{32}\frac{\hat{\Pi}_4^*}{\hat{\Pi}_1^*} + C_{12} \right\}^{(\bar{3})},
$$
$$
\left\langle zb_{11}^{(1)22} \right\rangle = \frac{1}{12} \left\{ C_{13}\frac{\hat{\Pi}_2}{\hat{\Pi}_1} + e_{31}\frac{\hat{\Pi}_3}{\hat{\Pi}_1} + Q_{31}\frac{\hat{\Pi}_4}{\hat{\Pi}_1} + C_{12} \right\}^{(\bar{3})}
$$
$$
\left\langle zb_{22}^{(1)22} \right\rangle = \frac{1}{12} \left\{ C_{23}\frac{\hat{\Pi}_2}{\hat{\Pi}_1} + e_{32}\frac{\hat{\Pi}_3}{\hat{\Pi}_1} + Q_{32}\frac{\hat{\Pi}_4}{\hat{\Pi}_1} + C_{22} \right\}^{(\bar{3})} +
$$
$$
+ \left\{ C_{12}\frac{\hat{\Pi}_6}{\hat{\Pi}_5} + C_{23}\frac{\hat{\Pi}_7}{\hat{\Pi}_5} + e_{32}\frac{\hat{\Pi}_8}{\hat{\Pi}_5} + Q_{32}\frac{\hat{\Pi}_9}{\hat{\Pi}_5} + C_{22} \right\}^{(\bar{1})} J_1^{(w)}
$$
$$
\left\langle zb_{12}^{(1)11} \right\rangle = \left\langle zb_{11}^{(1)12} \right\rangle = \left\langle zb_{12}^{(1)22} \right\rangle =
$$
$$
\left\langle zb_{22}^{(1)12} \right\rangle = \left\langle zb_{3j}^{\lambda\mu} \right\rangle = 0
$$

$$(4.27c)$$

and

$$
\left\langle zb_{12}^{(1)12} \right\rangle = \frac{1}{12} \{C_{66}\}^{(\bar{3})} + \frac{1}{12} \{C_{66}\}^{(\bar{1})} \left\{ \frac{H^3 t_1}{h_1} + \right.
$$
$$
\left. - K_1 \right\}^{(\bar{1})} + \frac{1}{12} \{C_{66}\}^{(\bar{2})} \left\{ \frac{H^3 t_2}{h_2} - K_2 \right\}^{(\bar{2})}
$$
$$
\text{where } K_1 = \frac{96 H^4}{\pi^5 h_1} \sqrt{\frac{\{C_{66}\}^{(\bar{1})}}{\{C_{44}\}^{(\bar{1})}}} \sum_{n=1}^{\infty} \frac{[1}{n^5} -
$$
$$
+ \frac{(-1)^n]}{n^5} \tanh \left(\sqrt{\frac{\{C_{44}\}^{(\bar{1})}}{\{C_{66}\}^{(\bar{1})}}} \frac{n\pi t_1}{2H} \right),
$$
$$
\text{and } \quad K_2 = \frac{96 H^4}{\pi^5 h_2} \sqrt{\frac{\{C_{66}\}^{(\bar{2})}}{\{C_{55}\}^{(\bar{2})}}} \sum_{n=1}^{\infty} \frac{[1}{n^5} -
$$
$$
+ \frac{(-1)^n]}{n^5} \tanh \left(\sqrt{\frac{\{C_{55}\}^{(\bar{2})}}{\{C_{66}\}^{(\bar{2})}}} \frac{n\pi t_2}{2H} \right).
$$

$$(4.27d)$$

As mentioned above, because the materials of choice in this example are orthotropic with the poling/magnetization direction chosen as the z-axis, the $\tau_{ij}^{(1)12}$ problem decouples from its $\tau_i^{(1)12}$, $\pi_i^{(1)12}$ counterparts. Therefore, the elastic coefficients in Eqs. 4.26c and 4.26d depend only on elastic parameters. Thus, for the $\left\langle zb_{12}^{(1)12} \right\rangle$ coefficient alone, the expression in Eq. 4.27d matches exactly the corresponding expression in Kalamkarov [45], Kalamkarov and Georgiades [60], Georgiades and Kalamkarov [61].

Using Eqs. 4.26d as well as Eqs. 4.7, 4.10, 4.13, 4.14a – 4.14c, 4.15a – 4.15c, 4.23a – 4.23c, 4.24a – 4.24c, 4.26a – 4.26d and (I-6.3), the effective in-plane, $\left\langle \delta_\alpha^{\mu\nu} \right\rangle$, and out-of-plane, $\left\langle \delta_\alpha^{(1)\mu\nu} \right\rangle$, piezoelectric coefficients, and the effective in-plane, $\left\langle \hat{a}_\alpha^{\mu\nu} \right\rangle$, and out-of-plane, $\left\langle a_\alpha^{(1)\mu\nu} \right\rangle$, piezomagnetic coefficients of the magnetoelectric wafer are obtained as follows:

$$
\left\langle \eta_\alpha^{\mu\nu} \right\rangle = \left\langle \delta_\alpha^{\mu\nu} \right\rangle = \left\langle a_\alpha^{(1)\mu\nu} \right\rangle = \left\langle \delta_\alpha^{(1)\mu\nu} \right\rangle = 0 \qquad (4.28)
$$

We observe in this example that the piezoelectric and piezomagnetic functions are zero. Clearly, this is because the polarization/magnetization directions were chosen to coincide with the z-axis for all three elements of the unit cell. Hence, the piezoelectric e_{11}, e_{12}, e_{13}, e_{21}, e_{22}, e_{23} values as well as the corresponding piezomagnetic values are zero for each constituent in each element. Had we chosen the poling/magnetization direction in, say, element Ω_1 to be parallel to y_1 and in element Ω_2 to be parallel to y_2, then the e_{11}, e_{12}, e_{13} piezoelectric and corresponding piezomagnetic coefficients would be non-zero in Ω_1, and likewise the e_{21}, e_{22}, e_{23} piezoelectric and corresponding piezomagnetic coefficients would be non-zero in Ω_2. Thus, the effective in-plane and out-of-plane piezoelectric

and piezomagnetic coefficients would be non-zero. As with the previous example, this underlines one of the principal advantages of our model; the designer has complete flexibility to enhance, reduce or even suppress selected coefficients to conform to the design criteria of a particular application, by changing one or more geometric, physical or material parameters.

(c) Unit-Cell Problems 2.4b, 2.5b and 2.6b and Effective Dielectric Permittivity, Magnetoelectric and Piezoelectric coefficients

We follow the same methodology as outlined above. For the sake of brevity we give only the final expressions.

$$
\begin{aligned}
-\langle \delta_{11} \rangle &= \left\{ \varepsilon_{11} + \frac{e_{15}^2}{C_{55}} \right\}^{(\bar{3})} + \left\{ \varepsilon_{11} + \frac{e_{15}^2}{C_{55}} \right\}^{(\bar{2})} F_2^{(w)} \\
-\langle \delta_{22} \rangle &= \left\{ \varepsilon_{22} + \frac{e_{24}^2}{C_{44}} \right\}^{(\bar{3})} + \left\{ \varepsilon_{22} + \frac{e_{24}^2}{C_{44}} \right\}^{(\bar{1})} F_1^{(w)}, \quad (4.29a) \\
\langle \delta_{12} \rangle &= \langle \delta_{21} \rangle = 0
\end{aligned}
$$

$$
\begin{aligned}
-\langle a_{11} \rangle &= \left\{ \lambda_{11} + \frac{e_{15}Q_{15}}{C_{55}} \right\}^{(\bar{3})} + \left\{ \lambda_{11} + \frac{e_{15}Q_{15}}{C_{55}} \right\}^{(\bar{2})} F_2^{(w)} \\
-\langle a_{22} \rangle &= \left\{ \lambda_{22} + \frac{e_{24}Q_{24}}{C_{44}} \right\}^{(\bar{3})} + \left\{ \lambda_{22} + \frac{e_{24}Q_{24}}{C_{44}} \right\}^{(\bar{1})} F_1^{(w)}, \\
\langle a_{12} \rangle &= \langle a_{21} \rangle = 0
\end{aligned}
$$

(4.29b)

$$
\langle b_\alpha^{\mu\nu} \rangle = 0 \qquad (4.29c)
$$

Eqs. 4.29a give the effective dielectric permittivity coefficients, Eqs. 4.29b give the first product properties we encounter, the effective magnetoelectric coefficients, and Eqs. 4.29c give the effective piezoelectric coefficients, which vanish for reasons explained above.

(d) Unit-Cell Problems 2.4c, 2.5c and 2.6c and Effective Magnetic Permeability, Magnetoelectric and Piezomagnetic Coefficients

As above, the effective magnetic permeability, magnetoelectric and piezomagnetic coefficients are given by Eqs. 4.30a, 4.30b and 4.30c respectively.

$$
\begin{aligned}
-\langle \gamma_{11} \rangle &= \left\{ \mu_{11} + \frac{Q_{15}^2}{C_{55}} \right\}^{(\bar{3})} + \left\{ \mu_{11} + \frac{Q_{15}^2}{C_{55}} \right\}^{(\bar{2})} F_2^{(w)} \\
-\langle \gamma_{22} \rangle &= \left\{ \mu_{22} + \frac{Q_{24}^2}{C_{44}} \right\}^{(\bar{3})} + \left\{ \mu_{22} + \frac{Q_{24}^2}{C_{44}} \right\}^{(\bar{1})} F_1^{(w)}, \\
\langle \gamma_{12} \rangle &= \langle \gamma_{21} \rangle = 0
\end{aligned}
$$

(4.30a)

$$
\begin{aligned}
-\langle \xi_{11} \rangle &= \left\{ \lambda_{11} + \frac{e_{15}Q_{15}}{C_{55}} \right\}^{(\bar{3})} + \left\{ \lambda_{11} + \frac{e_{15}Q_{15}}{C_{55}} \right\}^{(\bar{2})} F_2^{(w)} \\
-\langle \xi_{22} \rangle &= \left\{ \lambda_{22} + \frac{e_{24}Q_{24}}{C_{44}} \right\}^{(\bar{3})} + \left\{ \lambda_{22} + \frac{e_{24}Q_{24}}{C_{44}} \right\}^{(\bar{1})} F_1^{(w)}, \\
\langle \xi_{12} \rangle &= \langle \xi_{21} \rangle = 0
\end{aligned}
$$

(4.30b)

$$
\langle a_\alpha^{\mu\nu} \rangle = 0 \qquad (4.30c)
$$

Note that the effective magnetoelectric coefficients can be determined via two unit cell problems, and as expected $\langle \xi_{\alpha\mu} \rangle = \langle a_{\alpha\mu} \rangle$ in this case.

(e) Unit Cell Problems 2.4d, 2.5d and 2.6d and Effective Thermal Expansion, Pyroelectric and Pyromagnetic coefficients

The effective thermal expansion, pyromagnetic and pyroelectric coefficients are given by Eqs. 4.31a, 4.31b and 4.31c, respectively. We reiterate that these effective coefficients are related to the mid-plane component of the temperature variation, see Eq. (I-3.4b).

$$
\begin{aligned}
-\langle b_{11} \rangle &= \left\{ -C_{13} \frac{\hat{\Pi}_2^{\star(\Theta)}}{\hat{\Pi}_1^{\star(\Theta)}} - e_{31} \frac{\hat{\Pi}_3^{\star(\Theta)}}{\hat{\Pi}_1^{\star(\Theta)}} - Q_{31} \frac{\hat{\Pi}_4^{\star(\Theta)}}{\hat{\Pi}_1^{\star(\Theta)}} \right. \\
&\quad \left. + \Theta_{11} \right\}^{(\bar{3})} + \left\{ -C_{12} \frac{\hat{\Pi}_6^{\star(\Theta)}}{\hat{\Pi}_5^{\star(\Theta)}} - C_{13} \frac{\hat{\Pi}_7^{\star(\Theta)}}{\hat{\Pi}_5^{\star(\Theta)}} \right. \\
&\quad \left. - e_{31} \frac{\hat{\Pi}_8^{\star(\Theta)}}{\hat{\Pi}_5^{\star(\Theta)}} - Q_{31} \frac{\hat{\Pi}_9^{\star(\Theta)}}{\hat{\Pi}_5^{\star(\Theta)}} + \Theta_{11} \right\}^{(\bar{2})} F_2^{(w)} \\
-\langle b_{22} \rangle &= \left\{ -C_{23} \frac{\hat{\Pi}_2^{(\Theta)}}{\hat{\Pi}_1^{\star(\Theta)}} - e_{32} \frac{\hat{\Pi}_3^{(\Theta)}}{\hat{\Pi}_1^{\star(\Theta)}} - Q_{32} \frac{\hat{\Pi}_4^{(\Theta)}}{\hat{\Pi}_1^{\star(\Theta)}} \right. \\
&\quad \left. + \Theta_{22} \right\}^{(\bar{3})} + \left\{ -C_{12} \frac{\hat{\Pi}_6^{(\Theta)}}{\hat{\Pi}_5^{(\Theta)}} - C_{23} \frac{\hat{\Pi}_7^{(\Theta)}}{\hat{\Pi}_5^{(\Theta)}} \right. \\
&\quad \left. - e_{32} \frac{\hat{\Pi}_8^{(\Theta)}}{\hat{\Pi}_5^{(\Theta)}} - Q_{32} \frac{\hat{\Pi}_9^{(\Theta)}}{\hat{\Pi}_5^{(\Theta)}} + \Theta_{11} \right\}^{(\bar{1})} F_1^{(w)} \\
\langle b_{12} \rangle &= \langle b_{21} \rangle = 0
\end{aligned}
$$

(4.31a)

$$
\begin{aligned}
\langle \gamma_1 \rangle &= \{ \eta_1 \}^{(\bar{3})} + \{ \eta_1 \}^{(\bar{2})} F_2^{(w}, \\
\langle \gamma_2 \rangle &= \{ \eta_2 \}^{(\bar{3})} + \{ \eta_2 \}^{(\bar{1})} F_1^{(w)}
\end{aligned}
$$

(4.31b)

$$
\begin{aligned}
\langle \tau_1 \rangle &= \{ \xi_1 \}^{(\bar{3})} + \{ \xi_1 \}^{(\bar{2})} F_2^{(w)}, \\
\langle \tau_2 \rangle &= \{ \xi_2 \}^{(\bar{3})} + \{ \xi_2 \}^{(\bar{1})} F_1^{(w)}
\end{aligned}
$$

(4.31c)

In Eq. 4.31a, material parameters $\hat{\Pi}_1^{\star(\Theta)}$-$\hat{\Pi}_9^{\star(\Theta)}$ are obtained from the corresponding $\hat{\Pi}_1^\star$-$\hat{\Pi}_9^\star$ parameters via the following substitutions:

$$
\begin{aligned}
C_{13} &\to -\Theta_{33}, \quad Q_{31} \to \eta_3, \quad e_{31} \to \xi_3, \\
C_{12} &\to -\Theta_{22}
\end{aligned}
$$

(4.31d)

Likewise, parameters $\hat{\Pi}_1^{(\Theta)}$-$\hat{\Pi}_9^{(\Theta)}$ are obtained from the corresponding $\hat{\Pi}_1$-$\hat{\Pi}_9$ parameters via the following substitutions:

$$
\begin{aligned}
C_{23} &\to -\Theta_{33}, \quad Q_{32} \to \eta_3, \quad e_{32} \to \xi_3, \\
C_{12} &\to -\Theta_{11}
\end{aligned}
$$

(4.31e)

(f) Unit Cell Problems 2.4e, 2.5e and 2.6e and Secondary Effective Thermal Expansion, Pyroelectric and Pyromagnetic Coefficients

The effective thermal expansion, pyromagnetic and pyroelectric coefficients related to the linear through-the-thickness variation of the temperature field are given by Eqs. 4.32a, 4.32b and 4.32c, respectively.

$$
-\left\langle b_{11}^{(1)} \right\rangle = -\langle z b_{11} \rangle = \left\{ -C_{12} \frac{\hat{H}_6^{*(\theta)}}{\hat{H}_5^{*(\theta)}} - C_{13} \frac{\hat{H}_7^{*(\theta)}}{\hat{H}_5^{*(\theta)}} \right.
$$
$$
\left. -e_{31} \frac{\hat{H}_8^{*(\theta)}}{\hat{H}_5^{*(\theta)}} -Q_{31} \frac{\hat{H}_9^{*(\theta)}}{\hat{H}_5^{*(\theta)}} + \Theta_{11} \right\}^{(\hat{2})} S_2^{(w)}
$$
$$
-\left\langle b_{22}^{(1)} \right\rangle = -\langle z b_{22} \rangle = \left\{ -C_{12} \frac{\hat{H}_6^{(\theta)}}{\hat{H}_5^{(\theta)}} - C_{23} \frac{\hat{H}_7^{(\theta)}}{\hat{H}_5^{(\theta)}} \right.
$$
$$
\left. -e_{32} \frac{\hat{H}_8^{(\theta)}}{\hat{H}_5^{(\theta)}} -Q_{32} \frac{\hat{H}_9^{(\theta)}}{\hat{H}_5^{(\theta)}} + \Theta_{11} \right\}^{(\hat{1})} S_1^{(w)} \qquad (4.32a)
$$
$$
\left\langle b_{12}^{(1)} \right\rangle = \left\langle b_{21}^{(1)} \right\rangle = 0
$$

$$
\left\langle \gamma_1^{(1)} \right\rangle = \langle z \gamma_1 \rangle = \{\eta_1\}^{(\hat{2})} S_2^{(w)},
$$
$$
\left\langle \gamma_2^{(1)} \right\rangle = \langle z \gamma_2 \rangle = \{\eta_2\}^{(\hat{1})} S_1^{(w)} \qquad (4.32b)
$$

$$
\left\langle \tau_1^{(1)} \right\rangle = \langle z \tau_1 \rangle = \{\xi_1\}^{(\hat{2})} S_2^{(w},
$$
$$
\left\langle \tau_2^{(1)} \right\rangle = \langle z \tau_2 \rangle = \{\xi_2\}^{(\hat{1})} S_1^{(w)} \qquad (4.32c)
$$

(g) Comparison With Other Works and Discussion

As mentioned previously, for the case of the purely elastic case the results of this model converge exactly to those of Kalamkarov [45], Kalamkarov and Kolpakov [46]. However, examination of Eqs. 4.27a – 4.27c, reveals that in the general case of a smart composite structure, the elastic coefficients are dependent on not only the elastic properties of the constituent materials, but also on the piezoelectric, piezomagnetic, magnetic permeability, dielectric permittivity and other parameters. The same holds true for the remaining effective coefficients. In a sense, the thermoelasticity, piezoelectricity and piezomagnetism problems are entirely coupled and the solution of one affects the solutions of the others. This is captured in the present papers, but not in previously published works. Thus, the results presented here represent an important refinement of previously established results such as those in Kalamkarov and Georgiades [60], Georgiades and Kalamkarov [61], Kalamkarov [74], Kalamkarov and Challagulla [75]. In essence, in these previous studies semi-coupled analyses of composite and reinforced plates are carried out and therefore the resulting expressions of the effective coefficients do not reflect the influence of many parameters such as the electric permittivity, magnetic permeability, primary magnetoelectricity etc. In the present work however, a fully coupled analysis is performed and as a consequence the expressions for the effective coefficients involve all pertinent material parameters. To the authors' best knowledge, this is the first time that completely coupled piezo-magneto-thermo-elastic effective coefficients of reinforced plates are presented and

analyzed. Of course, the semi-coupled approach is fairly accurate in predicting many of the effective coefficients but may err significantly in some instances such as in the prediction of some of the product properties. This is also evident in corresponding micromechanical models of three-dimensional structures. For example, the fully-coupled approach given in Hadjiloizi et al. [25, 26], predicts the effective coefficients accurately whereas the semi-coupled approach in Challagulla and Georgiades [76] does not predict correctly some of the effective product properties. It is however accurate in predicting many of the remaining effective coefficients. Finally, we reiterate that if applied to the case of simple laminates, such as the ones considered in Section 3, the work presented here represents an extension of the classical composite laminate theory (see e.g. [66, 67]) to piezo-magneto-thermo-elastic structures.
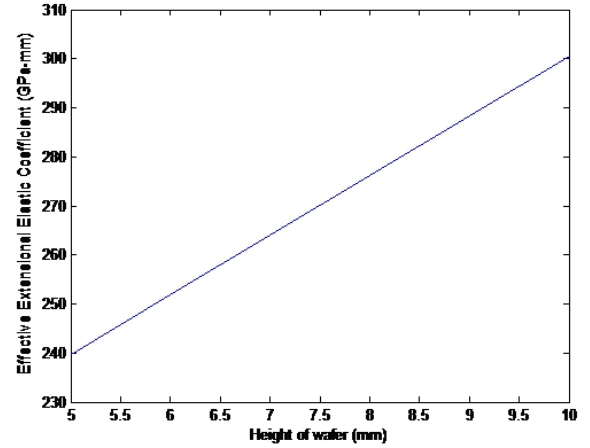
Figure 8: Plot of the effective $\left\langle b_{11}^{11} \right\rangle$ extensional coefficient vs. height of the piezoelectric wafer.

It is noted that the unit-cell problems are completely characterized by the structure of the unit cell of the magnetoelectric composite. It follows that the solutions of these problems and the effective coefficients in particular, are representative of the entire macroscopic composite and, once determined, they can be used to study a wide range of boundary value problems associated with that particular geometry. Examples include, but are certainly not limited to, static problems (the composite can be used as a structural member in manufacturing and infrastructure applications), dynamic problems (aerospace, automotive, vibration-absorption applications), magnetic/electric problems (the composites can be used as resonators, phase shifters, energy-harvesting devices, biomedical sensors and actuators), thermochem-

ical problems (chemical sensors) etc. Because the effective coefficients are representative of the macroscopic composite, the resulting expressions can easily be integrated in MATLAB^{TM} or other similar software packages to accurately and expediently analyze the aforementioned magnetoelectric structures. Ordinarily, the analysis and design of such complex geometries as shown in Fig. 6, would require a time-consuming numerical technique (such as the finite element method for example). The analytical model and its accompanying closed-form expressions presented here, however, allow us to quickly perform a preliminary design in a time-efficient manner. This preliminary design can then be used in conjunction with a finite element model to refine the results if enhanced accuracy is needed (by considering stress concentration effects for example). Obtaining a preliminary design before employing a numerical technique speeds up the design cycle time significantly. We finally note that the solutions of the local and the homogenized problems, Eqs. 2.3a- 2.3h, enable us to make very accurate predictions about the three-dimensional local structure of the mechanical displacements, electric and magnetic potentials, force and moment resultants, electric and magnetic displacements etc.
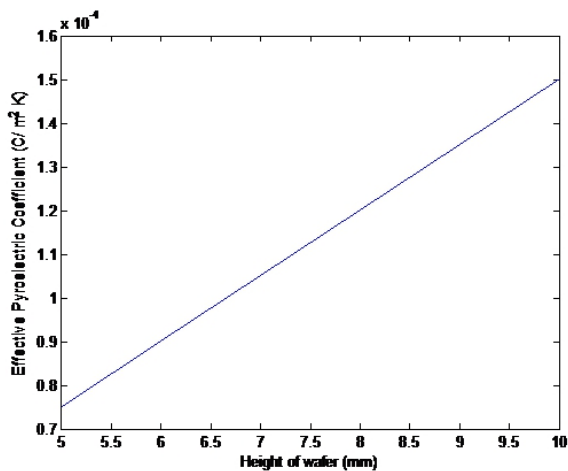

Figure 9: Plot of the effective $\langle \tau_1 \rangle$ pyroelectric coefficient vs. height of the piezoelectric wafer.

Before closing this section, let us examine a magnetoelectric wafer made up of a 1-mm-thick cobalt ferrite base plate and a barium titanate wafer with a thickness of 1 mm and height which varies from 5 to 10 mm. The material properties are taken from Table 1. Figs. 8 and 9 show, respectively, the effective extensional $\langle b_{11}^{11} \rangle$ coefficient and the effective pyroelectric $\langle \tau_1 \rangle$ coefficient. As expected, in-

creasing the height of the piezoelectric wafer increases the value of both coefficients.

5 Conclusions

The method of asymptotic homogenization was used to analyze a periodic smart composite magnetoelectric plate of rapidly varying thickness. From a set of eighteen unit cell problems the effective elastic, piezoelectric, magnetoelectric, pyromagnetic, thermal expansion and other coefficients for the homogenized anisotropic composite and/or reinforced plate were derived. These effective coefficients are universal in nature and may be utilized in studying very different types of boundary value problems associated with a given smart composite structure.

To illustrate the use of the unit cells and the applicability of the effective coefficients, two broad classes of examples were considered. The first example was concerned with a magnetoelectric laminate consisting of alternating piezoelectric and piezomagnetic laminae. The other example dealt with wafer-reinforced magnetoelectric plates. These are plates reinforced with mutually perpendicular ribs or stiffeners. The most general case was examined whereby the ribs had different orthotropic properties than the base plate. The unit cell problems were solved for this unique structure by considering each of the three regions of the unit cell separately. In the solution, we ignored complications at the regions of overlap between the actuators/reinforcements because these regions are highly localized and contribute very little to the integrals over the unit cell. The solution of the unit cell problems led to the determination of the effective coefficients including the product properties.

It is shown in this work that in the case of the purely elastic case, the results of the derived model converge exactly to those of Kalamkarov [45, 75], Kalamkarov and Kolpakov [46], Kalamkarov and Challagulla [76]. However, in the more general case wherein some or all of the phases exhibit piezoelectric and/or piezomagnetic behavior, the expressions for the derived effective coefficients were shown to be dependent on not only the elastic properties of the constituent materials, but also on the piezoelectric and piezomagnetic parameters.

One of the most important features of the derived model is that it affords complete flexibility to the designer to tailor the effective properties of the smart composite structure to conform to the requirements of a particular engineering application by changing one or more material or geometric parameters.

References

[1] Kalamkarov, A.L., Georgiades, A.V., MacDonald, D., and Fitzgerald, S., 2000, Pultruded FRP reinforcements with embedded fiber optic sensors, Canadian Journal of Civil Engineering, **27(5)**, pp. 972-984.

[2] A.K. Jain and J.S. Sirkis, Continuum damage mechanics in piezoelectric ceramics. Adaptive Structures and Composite Materials: Analysis and Application, Eds. E. Garcia, H. Cudney and A. Dasgupta, 47-58, (1994).

[3] Newnham R E, Skinner D P, Cross L E, Connectivity and piezoelectric-pyroelectric composites, Mat. Res. Bull. 13 (1978) 525-536.

[4] Nan C-W, Bichurin M I, Dong S, Viehland D and Srinivasan G Multiferroic magnetoelectric composites: Historical perspective, status, and future directions J. Appl. Phys 031101(1) – 031101 (2008) (35).

[5] Srinivasan G Magnetoelectric composites Annual Review of Materials Research, 40 (2010) 153-178.

[6] Bichurin M, Petrov V, Priya S, Bhalla A, Multiferroic magnetoelectric composites and their applications Advances in Condensed Matter Physics (2012) Article ID 129794.

[7] Bhatra D, Masud Md, De S K, Chauduri B K Large magnetoelectric effect and low-loss high relative permittivity in 0-3 CuO/PVDF composite films exhibiting unusual ferromagnetism at room temperature J. Phys. D: Appl. Phys. 45 (2012) 485002.

[8] Chen L, Li P, Wen Y, Zhu Y Analysis of the low-frequency magnetoelectric performance in three-phase laminate composites with Fe-based nanocrystalline ribbon Smart Materials and Structures 22 (2013) 115031

[9] Shen Y, Gao J, Hasanyan D, Wang Y, Li M, Li J, Viehland D Investigation of vehicle induced magnetic anomaly by triple-axis magnetoelectric sensors Smart Materials and Structures 21 (2012) 115007.

[10] Ju S, Chae S H, Choi Y, Lee S, Lee H W, Ji C-H A low frequency vibration energy harvester using magnetoelectric laminate composite Smart Materials and Structures 22 (2013) 115037.

[11] Ruy J, Priya S, Uchino K, Kim H-E Magnetoelectric effect in composites of magnetostrictive and piezoelectric materials Journal of Electroceramics 8 (2002) 107-119.

[12] Oh S R, Wong T C, Tan, C W, Yao K, Tay F E Fabrication of polymer multilayers on flexible substrates for energy harvesting Smart Materials and Structures 23 (2014) 015013.

[13] Lottermoser T, Lonkai T, Amann U, Hohlwein D, Ihringer J, Fiebig M Magnetic phase control by an electric field Nature 430 (2004) 541-544.

[14] Shen Y, McLaughlin K L, Gao J, Gray D, Shen L, Wang Y, Li M, Berry D, Li, J, Viehland D AC magnetic dipole localization by a magnetoelectric sensor Smart Materials and Structures 21

(2012) 065007.

[15] Harshe G, Doherty J P, Newnham RE Theoretical modeling of 3-0/0-3 magnetoelectric composites International Journal of Applied Electromagnetics in Materials, 4(2) (1993) 145-159

[16] Harshe G, Doherty J P, Newnham R E Theoretical modeling of multilayer magnetoelectric composites International Journal of Applied Electromagnetics in Materials 4(2) (1993) 161-171 .

[17] Avellaneda M, Harshé G Magnetoelectric effect in piezoelectric/magnetostrictive multilayer (2-2) composites J. Intel. Mat. Syst. Str. 5 (1994) 501-513.

[18] I.A. Osaretin, R.G. Rojas, Theoretical model for the magnetoelectric effect in magnetostrictive/piezoelectric composites, Phys. Rev. B 82 (2010) 174415(1)-174415(8).

[19] I. Getman, Magnetoelectric composite materials: Theoretical approach to determine their properties, Ferroelectrics 162(1) (1994), 45-50.

[20] C.W. Nan, Magnetoelectric effect in composites of piezoelectric and piezomagnetic phases, Physical Review B, 50(9), (1994), 6082-6088.

[21] Huang J H, Kuo W S The analysis of piezoelectric/piezomagnetic composite materials containing ellipsoidal inclusions Journal of Applied Physics 81(3) (1997) 1378-1386.

[22] Eshelby J D The determination of the elastic field of an ellipsoidal inclusion, and related problems Proc. R. Soc. Lond. A 241(1226) (1957) 376-396.

[23] Huang J H Analytical predictions for the magnetoelectric coupling in piezomagnetic materials reinforced by piezoelectric ellipsoidal inclusions Physical Review B 58(1) (1998) 12-15.

[24] Huang J H, Liu H K, Dai W L The optimized fiber volume fraction for magnetoelectric coupling effect in piezoelectric-piezomagnetic continuous fiber reinforced composites International Journal of Engineering Science **38**(11) (2000) 1207-1217.

[25] Hadjiloizi, D.A., Georgiades, A.V, Kalamkarov, A.L, Jothi, S, Micromechanical Model of Piezo-Magneto-Thermo-Elastic Composite Structures: Part I-Theory, European Journal of Mechanics A-Solids, **39**, (2013), 298-312.

[26] Hadjiloizi, D.A., Georgiades, A.V, Kalamkarov, A.L, Jothi, S, Micromechanical Model of Piezo-Magneto-Thermo-Elastic Composite Structures: Part II-Applications, European Journal of Mechanics A-Solids, **39**, (2013), 313-326.

[27] Bravo-Castillero J, Rodrigues-Ramos R, Mechkour H, Otero J, Sabina FJ Homogenization of magneto-electro-elastic multilaminated materials Q J Mechanics Appl Math 61(3) (2008) 311-332 .

[28] Ni Y, Priya S and Khachaturyan A G Modeling of magnetoelectric effect in polycrystalline multiferroic laminates influenced by the orientations of applied electric/magnetic fields J Appl Phys 105 (2009) 083914(1)-083914(4).

[29] C.H. Tsang, K.H. Chau, C.K. Wong, Y.W. Wong, F.G. Shin, Modeling of the magnetoelectric effect of three-phase multiferroic particulate composites, Integrated Ferroelectrics, 100:1, (2008), 177-197.

[30] D.A. Pan, S.G. Zhang, A.A. Volinsky, L.J. Qiao, Simple model of the magnetoelectric effect in layered cylindrical composites, J. Phys. D: Appl. Phys. 41 (2008) 205008(1)-205008(5).

[31] Bichurin M I, Petrov V N, Srinivasan G Modeling of magnetoelectric effect in ferromagnetic/piezoelectric multilayer composites Ferroelectrics 280 (2002) 165-175.

[32] Bichurin M I, Petrov V N, Averkin S V, Liverts E Present status of theoretical modeling the magnetoelectric effect in magnetostrictive-piezoelectric nanostructures. Part I: Low frequency electromechanical resonance ranges J. Appl. Phys. 107(5), (2010) 053904(1)-053904(11).

[33] Akbarzadeh A H, Babaei M H, Chen Z T The thermo-electromagnetoelastic behavior of a rotating functionally graded piezoelectric cylinder, Smart Mater. Struct. 20 (2011) 065008(1)- 065008(11).

[34] Soh A K, Liu J X On the constitutive equations of magnetoelectroelastic solids Journal of Intelligent Materials Systems and Structures 16 (2005) 597-602.

[35] Kirchner H O K, Alshits V I Elastically anisotropic angularly inhomogeneous media II. The Green's function for piezoelectric, piezomagnetic and magnetoelectric media Philosophical Magazine A 74(4) (1996) 861-885.

[36] Pan E, Heyliger R P Free vibrations of simply supported and multilayered magneto-electro-elastic plates, Journal of Sound and Vibration 252(3) (2002) 429-442.

[37] Benveniste Y, Milton G W New exact results for the effective electric, elastic, piezoelectric and other properties of composite ellipsoid assemblages Journal of the Mechanics and Physics of Solids 51(10) (2003) 1773-1813.

[38] Spyropoulos C P, Sih G C , Song Z F Magnetoelectroelastic composite with poling parallel to plane of line crack under out-of-plane deformation Theoretical and Applied Fracture Mechanics 40(2) (2003) 281-289.

[39] Tang T, Yu W Variational Asymptotic homogenization of heterogeneous electromagnetoelastic materials Int. J. Eng. Sci. 46 (2008) 741-757.

[40] Tang T, Yu W Micromechanical modeling of the multiphysical behavior of smart materials using the variational asymptotic method Smart Mater. Struct. 18(12) (2009) 125026 (1)-125026 (14).

[41] Bensoussan A, Lions J L, Papanicolaou G Asymptotic analysis for periodic structures, Amsterdam: North-Holland, 1978.

[42] Sanchez-Palencia E, Non-Homogeneous media and vibration theory. Lecture Notes in Physics, Berlin: Springer-Verlag, 1980.

[43] Bakhvalov N, Panasenko G Homogenisation: Averaging processes in periodic media, Amsterdam: Kluwer Academic Publishers, 1984.

[44] Cioranescu D, Donato P, An Introduction to homogenization ,Oxford: Oxford University Press, 1999.

[45] Kalamkarov A L, Composite and Reinforced Elements of Construction,New York: Wiley,1992.

[46] Kalamkarov A L, Kolpakov A G Analysis, design and optimization of composite structures ,New York: Wiley, 1997.

[47] Guedes J M and Kikuchi N Preprocessing and postprocessing for materials based on the homogenization method with adaptive finite element methods, Comput. Methods Appl. Mech. Engrg. 83 (1990) 143-198.

[48] Duvaut G Analyse fonctionnelle et méchanique des milieux continus, Proceedings of the 14th IUTAM Congress (Delft, Holland) (1976) 119-132.

[49] Duvaut G, Metellus A-M Homogénéisation d'une plaque mince en flexion de structure périodique et symétrique C.R. Acad. Sci., Ser. A. 283 (1976) 947-950.

[50] Andrianov I V, Manevich L I Shell design using the homogenization method Uspekhi Mekh 6 (1983) 3-29.

[51] Andrianov I V, Lesnichaya V , Manevich L I Homogenization methods in the statics and dynamics of ribbed shells (Moscow, Nauka) (1985).

[52] Caillerie D Equations de la diffusion stationnaire dans un domaine comportant une distribution périodique d'inclusions aplaties de grande conductivité C.R. Acad. Sci., Ser. 1 292(1) (1981) 115-118.

[53] Caillerie D Homogénéisation des equation de la diffusion stationnaire dans les domaines cylindrique aplatis Anal. Numér. 15 (1981) 295-319.

[54] Kohn R V, Vogelius M A new model for thin plates with rapidly varying thickness, Int. J. of Solids and Struct. 20 (1984) 333-350.

[55] Kohn R V, Vogelius M A new model for thin plates with rapidly varying thickness, II: A convergence proof, Quart. J. Appl. Math. 43 (1985) 1-22.

[56] Kohn R V, Vogelius M A new model for thin plates with rapidly varying thickness, III: Comparison of Different Scalings, Quart. J. Appl. Math. **44** (1986) 35-48.

[57] Hussain F, Hojjati M, Okamoto M, Gorga R.E., Polymer-matrix nanocomposites, processing, manufacturing and application: An overview, Journal of Composite Materials 40(17) (2006), 1511-1575.

[58] Challagulla K S, Georgiades A V, Kalamkarov A L Asymptotic homogenization modeling of smart composite generally orthotropic grid-reinforced shells. Part I-Theory European Journal of Mechanics A-Solids 29 (2010) 530-540.

[59] Georgiades A V, Challagulla K S, Kalamkarov A L Asymptotic homogenization modeling of smart composite generally orthotropic grid-reinforced shells. Part II-Applications European Journal of Mechanics A-Solids 29 (2010) 541-556.

[60] A.L. Kalamkarov and A.V. Georgiades, Asymptotic homogenization models for smart composite plates with rapidly varying thickness: Part I-Theory, Journal of Multiscale Computational Engineering **2**(1) (2004) 133-148.

[61] A.V. Georgiades and A.L. Kalamkarov, Asymptotic homogenization models for smart composite plates with rapidly varying thickness: Part II-Applications, Journal of Multiscale Computational Engineering **2**(1) (2004) 149-174.

[62] G.C. Saha, A.L. Kalamkarov, A.V. Georgiades, Micromechanical analysis of effective piezoelastic properties of smart composite sandwich shells made of generally orthotropic materials, Smart Materials and Structures 16(3) (2007) 866-883.

[63] Hadjiloizi D A, Georgiades A V, Kalamkarov A L. Dynamic modeling and determination of effective properties of smart composite plates with rapidly varying thickness, International Journal of Engineering Science 56 (2012) 63-85.

[64] Hadjiloizi D A, Kalamkarov A L, Georgiades A V, Quasi-static Analysis of Piezo-Magneto-Thermo-Elastic Composite and Reinforced Plates: Part I – Model Development, Curved and Layered Structures 1 (2014) 11-31.

[65] Sevostianov I, Kachanov M Effect of interphase layers on the overall elastic and conductive properties of matrix composites. Applications to nanosize inclusion Int. J. Solids Struct. 44 (2007) 1304-1315.

[66] Gibson R F, Principles of Composite Material Mechanics, McGraw-Hill, New York, 1994.

[67] Vinson, J R, Sierakowski, R L, The Behavior of Structures Composed of Composite Materials, Kluwer Academic Publishers, Dordrecht, Netherlands, 2002.

[68] Reddy, J N, Mechanics of laminated composite plates, CRC Press, New York, 1997.

[69] Li L, Dunn ML, Micromechanics of magnetoelectroelastic composite materials: average fields and effective behaviour, J. Intel. Mat. Syst. Str. 1998; 9: 404–416.

[70] Yoshihiro O, Tanigawa Y. Transient analysis of multilayered magneto-electro-thermoelastic strip due to nonuniform heat supply, Compos. Struct. 2005; 66: 471-480.

[71] Cook W R Jr, Berlincourt, D A, Scholz, Thermal Expansion and pyroelectricity in Lead Zirconium Titanate Zirconate and Barium Titanate, Journal of Applied Physics 34 (1963), 1392-1398.

[72] Verma KC, Gupta V, Kaur J, Kotnala, R K, Raman Spectra, photoluminescence, magnetism and magnetoelectric coupling in pure and Fe doped $BaTiO_3$ nanostructures, Journal of Alloys and Compounds 578 (2013), 5-11.

[73] Dascalu G, Popescu T, Feder, M, Caltun, O F, Structural, electric and magnetic properties of $CoFe_{1.8}RE_{0.2}O_4$ (RE = Dy, Gd, La) bulk materials, Journal of Magnetism and Magnetic Materials 33 (2013), 69-74.

[74] Kalamkarov, AL (2014) Asymptotic Homogenization Method and Micromechanical Models for Composite Materials and Thin-Walled Composite Structures, in "Mathematical Methods and Models in Composites," pp. 1-60, Imperial College Press, London.

[75] Kalamkarov, AL and Challagulla KS (2013) Effective Properties of Composite Materials, Reinforced Structures and Smart Composites. Asymptotic Homogenization Approach, in "Effective Properties of Heterogeneous Materials," Solid Mechanics and Its Applications, Vol. 193, pp. 283-363. Springer, Dordrecht, New York.

[76] Challagulla, KS, Georgiades AV. Micromechanical Analysis of Magneto-Electro-Thermo-Elastic Composite Materials with Applications to Multilayered Structures. International Journal of Engineering Science 49 (2011) 85-104.